

Demography-adjusted tests of neutrality based on genome-wide SNP data

M. Rafajlović^{a,d}, A. Klassmann^{b,d}, A. Eriksson^c, T. Wiehe^b, and B. Mehlig^a

^aDepartment of Physics, University of Gothenburg, SE-41296 Gothenburg, Sweden

^bInstitut für Genetik, Universität zu Köln, 50674 Köln, Germany

^cDepartment of Zoology, University of Cambridge, CB2 3EJ Cambridge, UK

^dThese authors have equally contributed to this work

Tests of the neutral evolution hypothesis are usually built on the standard null model which assumes that mutations are neutral and population size remains constant over time. However, it is unclear how such tests are affected if the last assumption is dropped. Here, we extend the unifying framework for tests based on the site frequency spectrum, introduced by Achaz and Ferretti, to populations of varying size. A key ingredient is to specify the first two moments of the frequency spectrum. We show that these moments can be determined analytically if a population has experienced two instantaneous size changes in the past. We apply our method to data from ten human populations gathered in the 1000 genomes project, estimate their demographies and define demography-adjusted versions of Tajima's D , Fay & Wu's H , and Zeng's E . The adjusted test statistics facilitate the direct comparison between populations and they show that most of the differences among populations seen in the original tests can be explained by demography. We carried out whole genome screens for deviation from neutrality and identified candidate regions of recent positive selection. We provide track files with values of the adjusted and original tests for upload to the UCSC genome browser.

Keywords: Single nucleotide polymorphism, infinite-sites model, site frequency spectrum, bottleneck, coalescent approximation.

I. INTRODUCTION

In natural populations, genetic diversity is shaped not only by population genetic forces such as drift and natural selection, but also by geographic structure and demographic history. Many statistical tests to identify genome regions affected by natural selection have been proposed in the past, such as iHS (Voight et al., 2006), $XP-EHH$ (Tang et al., 2007) as well as Tajima's D (Tajima, 1989a), Fay&Wu's H (Fay and Wu, 2000), and Zeng's E (Zeng et al., 2006). Tests of neutrality have frequently been used to search for signatures of selection in the human genome (Akey et al., 2004; Carlson et al., 2005; Nielsen et al., 2005; Stajich and Hahn, 2005; Voight et al., 2006). However, distinguishing selection from demographic effects in genomic data remains a challenge (Akey et al., 2004; Stajich and Hahn, 2005). In this paper, we focus on tests based on the shape of the site frequency spectrum, such as Tajima's D , Fay&Wu's H , and Zeng's E . As examples, we show in Fig. 1 (upper panels) genome-wide values of these tests for a European (CEU), Asian (CHB), and African human population (YRI) in the 1000 genomes project dataset (McVean et al., 2012). As Fig. 1 (upper panels) shows, the distributions of the tests differ substantially between different populations. To which extent do these differences arise from differences in demographic histories of the populations? In order to answer this question, it is necessary to eliminate the effects of demographies on the values of tests. In this study, we achieve this by adjusting the site frequency spectrum of tests of neutrality for the deviation of population demographies from constant size. Thus, we modify tests of neutrality by directly integrating demographies into them. We refer to such modified tests as *demography-adjusted*. When demography corresponds to constant population size, demography-adjusted tests reduce to the tests defined for the standard Wright-Fisher model, hereafter referred to as *original tests*.

The distributions of demography-adjusted tests are similar to the distributions of the corresponding original tests computed under the standard null model. Consequently, demography-adjusted tests significantly simplify a direct comparison of the values of tests between different populations by emphasising the relevant differences. Examples are given in Fig. 1 (lower panels), where we show the distributions of our demography-adjusted Tajima's D , Fay&Wu's H , and Zeng's E for the populations CEU, CHB, and YRI. As this figure suggests, most of the differences in the distributions of the tests between human populations arise from their distinct underlying demographies.

Since human demographies are unknown, it is necessary to estimate them. As suggested by Nielsen (2000) (see also Adams and Hudson (2004)), we apply a maximum likelihood method to genome-wide single nucleotide polymorphisms (SNPs). As an approximation for the demographies of human populations we use a simplified model with two instantaneous population size changes in the past, as proposed before (Adams and Hudson, 2004; Marth et al., 2004; Stajich and Hahn, 2005). This model is characterized by four unknown parameters. It has the appealing property to yield exact analytical expressions for the first two moments of the site frequency spectrum (SFS). These are required to formulate our demography-adjusted tests of neutrality and they are explicitly derived in this paper.

The error in the estimate of demographic parameters depends on the noise in the genome-wide SFS, thus on the number of SNPs used for the estimation. We analyse the sensitivity of demography-adjusted tests by using coalescent simulations. On the basis of two reference demographies with two population-size changes in the past, we determine the number of SNPs required for reliable adjustment of the tests.

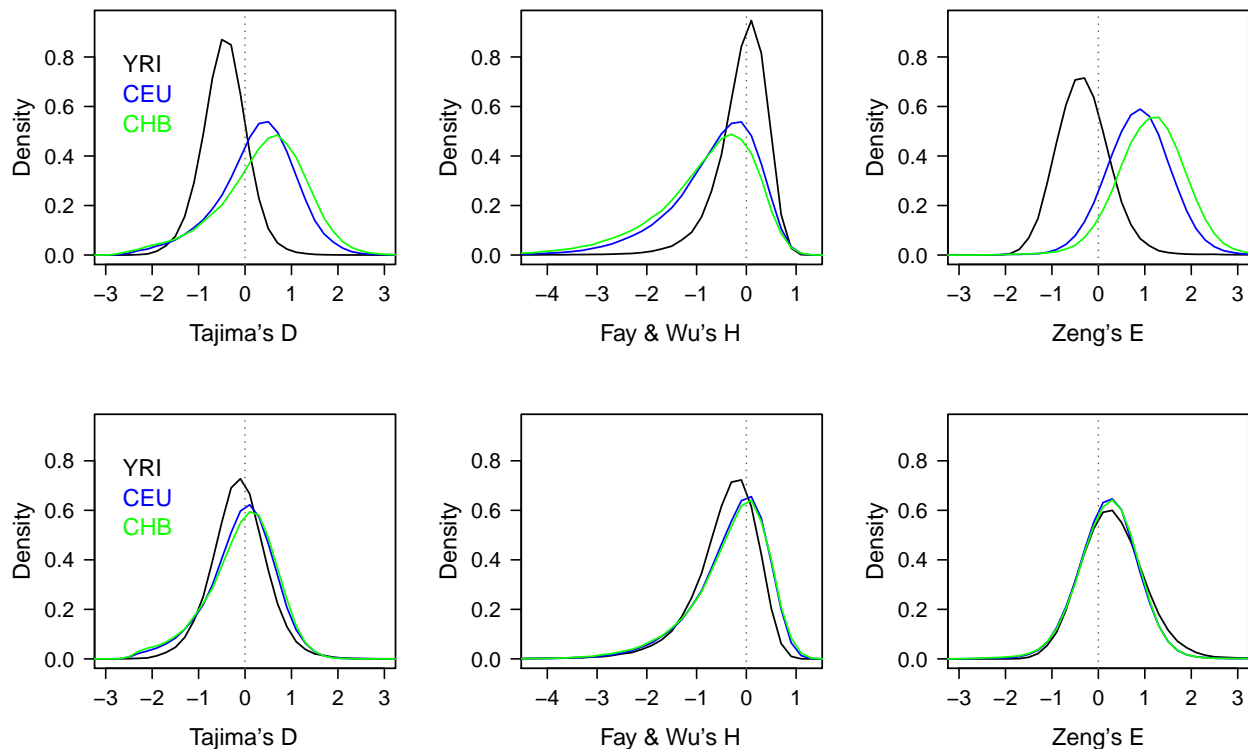


FIG. 1 Distribution of test values over all sliding windows. Top row: original tests. Bottom row: demography-adjusted tests.

The populations CEU, CHB, and YRI are only three exemplary populations chosen from a set of ten populations analysed in this study by means of demography-adjusted tests. Assuming a piecewise constant demographic model, we find that Europeans and Asians went through a recent population bottleneck, which is in agreement with Adams and Hudson (2004) and Marth et al. (2004). In contrast, the African populations either experienced two population-size expansions (ASW, again in agreement with Adams and Hudson (2004) and Marth et al. (2004)), or an ancient expansion, followed by a recent population-size decline (LWK, YRI).

Our results further show that demography-adjustment of SFS-based tests is essentially reflected in an affine linear transformation of the test statistic. Consequently, the genomic regions recognized to be under selection by the adjusted tests strongly overlap with the originally detected regions. However, our adjusted tests permit a direct comparison of results from different populations with different demographies.

We provide original and adjusted tests values as BED-files, formatted for upload to the UCSC genome browser.

II. MATERIALS AND METHODS

A. Demographic model

We assume a piecewise constant demography with two population-size changes in the past as illustrated in Fig. 2. When $N_2 < N_1$ and $N_2 < N_3$ the demography represents a population bottleneck. The model of piecewise constant demographies with two population-size changes in the past was considered before (Adams and Hudson, 2004; Marth et al., 2004; Stajich and Hahn, 2005) to capture the main events of the human out-of-Africa expansion (Cavalli-Sforza and Feldman, 2003; Eriksson et al., 2012; Liu et al., 2006; Ramachandran et al., 2005; Tanabe et al., 2010).

In the following we assume a random mating Wright-Fisher diploid population (Fisher, 1930; Wright, 1931). We also assume that the population size is large so that the standard coalescent approximation to the Wright-Fisher population can be used (Kingman, 1982).

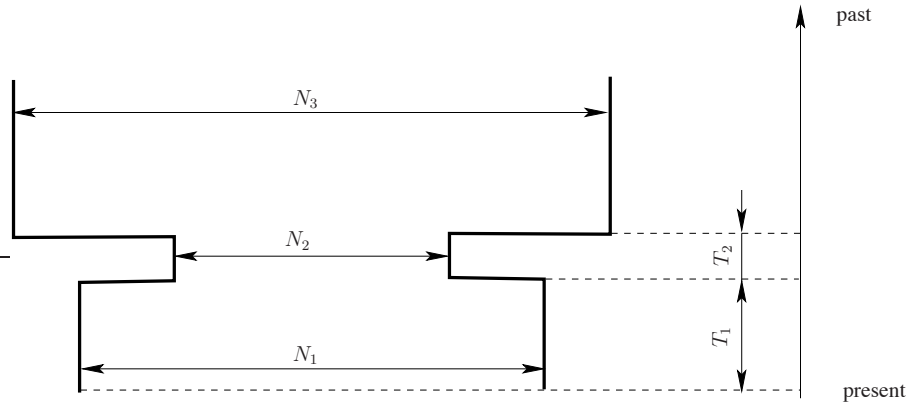


FIG. 2 Demographic model. Present population size is N_1 . In the past, two population-size changes occurred: one at T_1 generations ago from N_1 to N_2 and another one $T_1 + T_2$ generations ago from N_2 to N_3 .

B. Demography-adjusted tests of neutrality

Tajima (1989a) introduced a test of neutrality which compares two estimators of the scaled mutation rate $\theta = 4\mu LN$, with N denoting diploid population size, μ mutation rate per site, per chromosome, per generation, and L the number of sites in the genomic sequence. If mutations are neutral, these two estimators have the same expected values. A significant difference between them indicates a violation of the null assumptions, i.e. either the population size is varying, or mutations are not neutral (or both). Several other tests of neutrality, relying on the same idea and on the same null model, have been proposed since (Fu and Li (1993b), Fay and Wu (2000), Zeng et al. (2006), Achaz (2008)). Achaz (2009) showed that estimators of θ in any of these tests can be expressed as linear combinations of the SFS, and as instances of a single general formula (see Eq. (8) in Achaz (2009)).

We show that this can be further generalised to include demographies with varying population size. Following the notation introduced by Achaz (2009) and Ferretti et al. (2010), we write the null site frequency spectrum in the form $\langle \xi_i \rangle = \xi_i^0 \theta$. Here $\xi_i^0 = \langle \xi_i \rangle|_{\theta=1}$ is the expected total branch length of lineages in the gene genealogical tree of the sample that have exactly i leafs. It depends on the sample size n and the parameters of the demography, but not on θ . It follows that in a sample of size n , the SFS provides $n - 1$ unbiased estimators $\hat{\theta}^{(i)} = \xi_i / \xi_i^0$. In fact, any linear combination of $\hat{\theta}^{(i)}$ can be used as an estimator of θ :

$$\hat{\theta}_\omega = \sum_{i=1}^{n-1} \omega_i \hat{\theta}^{(i)}, \quad (1)$$

where ω_i are the weights satisfying $\sum_i \omega_i = 1$. All tests mentioned above compare two different such estimators and are determined only by the difference $\Omega_i = \omega_i^{(1)} - \omega_i^{(2)}$ of the corresponding weights (listed in Table 1 and 2 of Achaz (2009)).

It follows from Eq. (1) that a demography-adjusted test of neutrality, denoted by T_Ω below, takes the form (Ferretti et al., 2010, their suppl. Eq. (20)):

$$T_\Omega = \frac{\sum_{i=1}^{n-1} \Omega_i \hat{\theta}^{(i)}}{\sqrt{\text{Var} \left[\sum_{i=1}^{n-1} \Omega_i \hat{\theta}^{(i)} \right]}}. \quad (2)$$

The denominator in Eq. (2) for a constant population size is given by Achaz (2009, his Eq. (9)). For a varying population size, we calculate analogously (see Appendix IV):

$$\text{Var} \left[\sum_{i=1}^{n-1} \Omega_i \hat{\theta}^{(i)} \right] = \theta \sum_{i=1}^{n-1} \frac{\Omega_i^2}{\xi_i^0} + \theta^2 \sum_{i,j=1}^{n-1} \frac{\Omega_i}{\xi_i^0} \sigma_{ij}^0 \frac{\Omega_j}{\xi_j^0}, \quad (3)$$

where $\sigma_{ij}^0 = \text{Cov}(\xi_i, \xi_j)|_{\theta=1}$ for $i \neq j$, and $\sigma_{ii}^0 = (\text{Var}(\xi_i) - \langle \xi_i \rangle^2)|_{\theta=1}$, as defined in Fu (1995). Note that, according to its definition, σ_{ij}^0 does not depend on θ . In the constant population-size case, it is a function of sample size n (see Fu (1995)), and for a non-constant demography it is a function of n and of the parameters of the demography.

As Eq. (3) shows, an estimate of θ and of θ^2 is needed to calculate the variance. Tajima (1989a) used the estimator $\hat{\theta}_S =$

$\frac{1}{\sum_{k=1}^{n-1} \frac{1}{k}} \sum_{i=1}^{n-1} \xi_i = \frac{1}{\sum_{k=1}^{n-1} \frac{1}{k}} S$ (where $S = \sum_{i=1}^{n-1} \xi_i$ is the number of segregating sites). We extend this definition to an arbitrary null spectrum by setting $\hat{\theta}_S = \frac{1}{\sum_{k=1}^{n-1} \xi_k^0} S$. We find that an unbiased estimate of θ^2 based on $\hat{\theta}_S$ is given by (see Appendix IV)

$$\widehat{\theta}_S^2 = \frac{\hat{\theta}_S^2 - y_n \hat{\theta}_S}{1 + z_n}. \quad (4)$$

Here, y_n and z_n are given by

$$y_n = \left(\sum_{i=1}^{n-1} \xi_i^0 \right)^{-1} \text{ and } z_n = \left(\sum_{i,j=1}^{n-1} \sigma_{ij}^0 \right) \left(\sum_{i=1}^{n-1} \xi_i^0 \right)^{-2}. \quad (5)$$

For constant population size y_n and z_n reduce to

$$y_n = \left(\sum_{i=1}^{n-1} \frac{1}{i} \right)^{-1} \text{ and } z_n = \sum_{i=1}^{n-1} \frac{1}{i^2} \left(\sum_{i=1}^{n-1} \frac{1}{i} \right)^{-2}. \quad (6)$$

It is known that estimation of θ by $\hat{\theta}_S$ is efficient (i.e. the estimator has minimal variance) for small values of θ (Fu and Li, 1993a). One can show that this holds for our extended version of $\hat{\theta}_S$ as well. In fact, the estimator can become efficient even for high values of θ , if recombination is taken into account. We note that it is common practise to apply tests, such as Tajima's D , to recombining sequences (Akey et al., 2004; Carlson et al., 2005; Stajich and Hahn, 2005) although their derivation neglects recombination.

In our genome scan we encounter rather high values of θ in the range of 50 – 100. In this case the first summand in Eq. (3) can be neglected. Hence, Eq. (2) can be approximated by

$$T_\Omega \approx \frac{\sum_{i=1}^{n-1} \frac{\Omega_i \xi_i}{\xi_i^0}}{\frac{1}{\sum_{i=1}^{n-1} \xi_i^0} S \sqrt{\sum_{i,j=1}^{n-1} \frac{\Omega_i \sigma_{ij}^0 \Omega_j}{\xi_i^0 \xi_j^0}}} \quad (7)$$

and the adjustment of the tests to demography with varying population size can be interpreted as a combination of a modified weighting (via ξ_i^0) and scaling (via ξ_i^0 and σ_{ij}^0), yielding an affine linear transformation.

Note, that our adjusted tests co-incide with the original ones if population size is constant. In this case, expressions for ξ_i^0 and σ_{ij}^0 have been explicitly derived by Fu (1995). In case of varying population size, the corresponding expressions are, in general, unknown. For a piecewise constant demography, Marth et al. (2004) derived an expression for the first moment of the SFS. In this study, we use results of Fu (1995) and of Eriksson et al. (2010) (see also Zivkovic and Wiehe (2008)) to compute the second moment of the SFS under a piecewise constant demography shown in Fig. 2. We remark, that this can be done in the same way for the folded SFS (FSFS), i.e. when data cannot be polarized. The details and the corresponding formulae for the demographic model shown in Fig. 2 are given in Appendix IV.

C. Estimating demographic parameters using the SFS

We use the analytical expressions for the moments of the SFS under a given demography to compute maximum likelihood (ML) estimates of the parameters of our demographic model. We follow a similar approach as described in Adams and Hudson (2004), namely we calculate the expected SFS for a large set of plausible parameters and choose the parameters with highest likelihood, given the data. If SNPs are assumed to be uncorrelated, the SFS counts ξ_1, \dots, ξ_{n-1} are multinomially distributed (conditional on the total number of SNPs $S = \sum_{i=1}^{n-1} \xi_i$), with the parameters given by the expected values of ξ_i (Adams and Hudson, 2004; Nielsen, 2000).

Similarly, the probability to observe the FSFS $\eta_1, \dots, \eta_{\lfloor n/2 \rfloor}$ in a sample of $S = \sum_{i=1}^{\lfloor n/2 \rfloor} \eta_i$ polymorphic sites is multinomial with

$$\text{Prob}(\eta_1, \eta_2, \dots, \eta_{\lfloor n/2 \rfloor} | S) = \binom{S}{\eta_1, \eta_2, \dots, \eta_{\lfloor n/2 \rfloor}} \prod_{i=1}^{\lfloor n/2 \rfloor} p_i^{\eta_i}. \quad (8)$$

TABLE I Populations and the corresponding number of individuals sampled (data from the 1000 genomes project (McVean et al., 2012)).

	Population	Sample
CEU	CEPH individuals	85
FIN	Finnish in Finland	93
GBR	British from England and Scotland	89
TSI	Tosceni in Italia	98
CHB	Han Chinese in Beijing, China	97
CHS	Han Chinese South, China	100
JPT	Japanese in Tokyo, Japan	89
ASW	African ancestry in Southwest USA	61
LWK	Luhya in Webuye, Kenya	97
YRI	Yoruba in Ibadan, Nigeria	88

In this case, the parameters p_i are given by:

$$p_i = \frac{\langle \eta_i \rangle}{\sum_{j=1}^{\lfloor n/2 \rfloor} \langle \eta_j \rangle}. \quad (9)$$

As mentioned in the previous subsection, the expression for $\langle \xi_i \rangle$ (and thus for $\langle \eta_i \rangle$) under the model shown in Fig. 2 is given in Appendix IV.

It is known that different demographies can lead to exactly the same SFS (Myers et al., 2008). Hence, cases exist in which it is difficult to distinguish the underlying demographies by their spectra. In order to obtain an estimate for the minimum number of SNPs necessary for reliable inference, we use coalescent simulations to generate SFSs under two different demographic histories with two population-size changes in the past (see Fig. 3). Reconstruction of the ancestral allele via an outgroup is prone to mis-specification, which can substantially bias demography estimation. We therefore used the folded SFSs (FSFSs) for demography estimation, which is independent of the ancestral allele. We simulated $81 \cdot 10^6$ independent gene genealogies with $n = 60$, and $\theta = 0.01$. For such a small value of θ , genealogies rarely contain more than one mutation. For each demography, we determine three resulting FSFSs, one containing 10^4 SNPs, one with 10^5 SNPs, and one with 10^6 SNPs (see circles in Fig. S1 in Supplementary material). To obtain the FSFSs in a way consistent with practical data sampling, we randomly select exactly one SNP from randomly chosen genealogies having mutations. Using such spectra, we compute ML-parameters of demographies with two population-size changes in the past. We note that, under the model considered, there are four unknown parameters to be determined. Upon scaling the parameters of the model (N_1, N_2, N_3, T_1, T_2) by the present population size N_1 , the unknown parameters actually are the scaled population sizes $x_i = N_i/N_1$ ($i = 2, 3$), and the scaled times t_i such that $T_i = \lfloor 2t_i N_1 \rfloor$ ($i = 1, 2$). For the given parameters x_2, x_3, t_1 , and t_2 , the probabilities p_i can be computed using Eqs. (22)-(24) in Appendix IV. Note that the ML-estimation does not depend on the parameter θ , as Eq. (9) shows. The ML-demographies are found by computing $\text{Prob}(\eta_1, \dots, \eta_{\lfloor n/2 \rfloor} | S_n)$ for a set of candidate parameters: the logarithms of candidate population sizes x_2 , and x_3 are taken from a grid within the interval $[-2, 2]$, and the logarithms of candidate times t_1 , and t_2 are taken from a grid within the interval $[-3, 0]$ (in both cases successive points are equally spaced by 0.025 units). Thus, for each population we test in total $121^2 \cdot 161^2 = 379,509,361$ combinations of the four unknown demographic parameters. The results are shown in Section III.

We apply this procedure to the FSFSs of ten human populations (see Table I) to estimate the parameters of the corresponding piecewise constant demographies with two population-size changes in the past (Fig. 2). Data were taken from the 1000 genomes project (McVean et al., 2012), version 3 of the release of integrated variant calls from April 30th, 2012. Variants were filtered by variant type ‘‘SNP’’ (i.e. indels excluded). From each population, four (possibly overlapping) subsamples of 30 individuals were drawn. We used only SNPs from intergenic regions.

As explained above, in order to use the analytical formulae for parameter estimation, SNPs must be uncorrelated, i.e. unlinked. On the other hand, a large amount of SNPs is necessary to render the demography estimation reliable. As a compromise we collect the SNPs in the following way: from each of the 4 subsamples of 30 individuals we draw randomly 10^4 SNPs with the condition that the minimal physical distance between any pair of SNPs is $5 \cdot 10^4$ base pairs (50 kb). This is repeated 10 times for each subsample to obtain in total 40 random spectra. We perform the ML-estimation for each population by using the average of these 40 spectra. Results are shown in Section III.

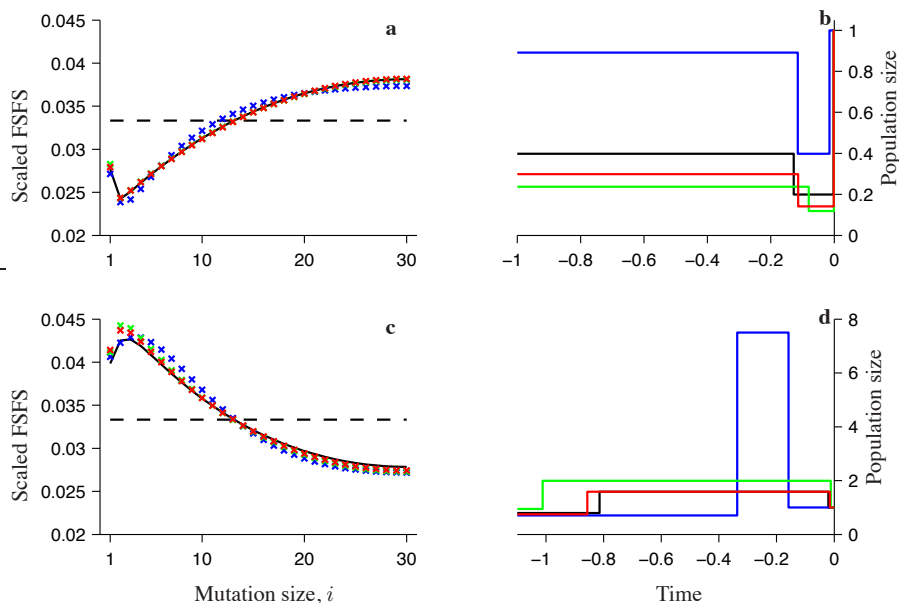


FIG. 3 (a), (c) Scaled FSFSs computed analytically. The spectra are scaled so that, in the constant population-size case, one obtains a constant equal to $1/\lfloor n/2 \rfloor$ (shown by dashed lines). Analytical spectra corresponding to the actual underlying demographies (shown by black lines in panels **b** and **d**, respectively) are shown by black lines. The best-fitted spectra estimated using 10^4 SNPs, green crosses show the best-fitted spectra estimated using 10^5 SNPs, and red crosses show the best-fitted spectra estimated using 10^6 SNPs. (b) Actual underlying demography (black line) for the spectrum shown in **a** by a black line (recent bottleneck). (d) Actual demography (black line) for the spectrum shown in **c** by a black line (past population-size expansion, followed by a recent population-size decline). In **b** and **d** the maximum likelihood histories estimated using 10^4 SNPs, 10^5 SNPs, and 10^6 SNPs are shown by blue, green, and red lines, respectively. The population size is scaled by N_1 , and the time is scaled by $2N_1$. Sample size used: $n = 60$.

D. Whole-genome scans with demography-adjusted tests of neutrality

First, we investigate with simulations the error introduced by demography inference. We simulate 10^6 independent gene genealogies under two idealized demographies roughly representing the populations CEU and YRI, shown in Fig. 3**b**, **d** by black lines (recent bottleneck in **b**, and past population-size expansion followed by a recent decline in **d**). We performed coalescent simulations with $\theta = 100$, corresponding to the values in our genome scan. For each gene genealogy, we compute the distribution of Tajima's D adjusted to the actual demography, as well as to the estimated demography, and we compare the two.

We perform genome wide computation of Tajima's D , Fay & Wu's H and Zeng's E using the approach by Carlson et al. (2005). We calculate the tests in a sliding window of size 100 kb and step size 10 kb. Windows containing less than 5 SNPs were ignored and we collected about 280,000 data points. For the tests of Fay & Wu, and of Zeng it is necessary to know the ancestral allele. This information was obtained through a 6-way alignment of humans and five other primates and is included into the 1000 genomes data. In order to detect putative regions under selection, we distinguished so-called "contiguous regions of Tajima's D reduction (CRTR)". As in Carlson et al. (2005) we define them as a genomic region of at least 20 consecutive windows, of which at least 75 % show a Tajima's D belonging to the 1% lowest overall values.

III. RESULTS

A. Test of the maximum likelihood procedure

In Fig. 3**a**, **c** we show by black lines the analytically computed scaled FSFSs under a recent bottleneck (**a**), that is under a past population-size expansion followed by a recent decline (**c**). The spectra are scaled so that in the constant population-size case one obtains a constant value (independent of i) equal to $1/\lfloor n/2 \rfloor$ (dashed lines in Fig. 3**a**, **c**). The demography estimation is based on the spectra obtained using coalescent simulations with 10^4 , or 10^5 , or 10^6 SNPs (see blue, green, and red circles in Fig. S1**b**, **d** in Supplementary material). By comparing the actual underlying histories to the estimated ones, we find that our ML-procedure works well when using spectra with $\geq 10^5$ SNPs.

In Fig. 4 we show the distributions of Tajima's D adjusted to the ML-demographies shown in Fig. 3**b**, **d** (blue, and green

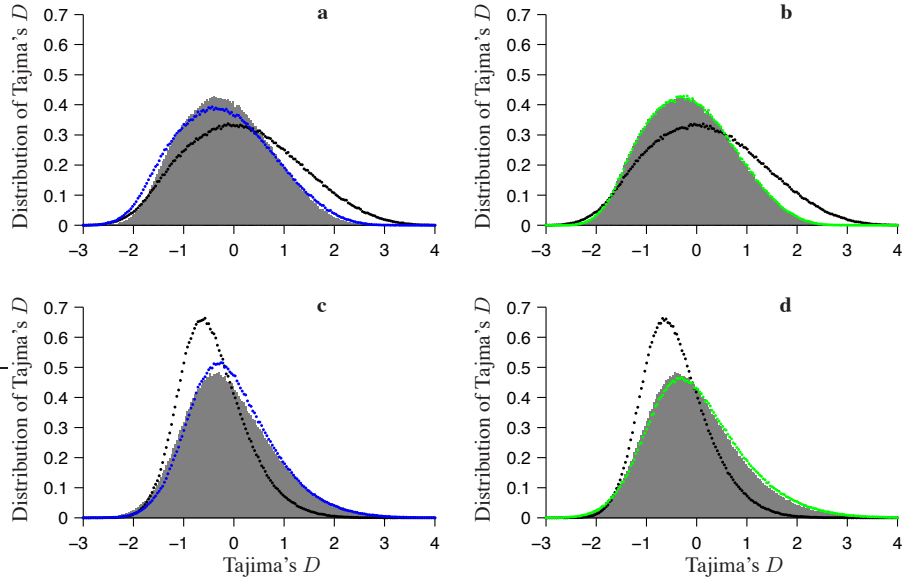


FIG. 4 (a), (b) Numerically computed distributions of Tajima's D for demographic histories shown in Fig. 3b. Grey region shows the distribution of Tajima's D adjusted to the actual underlying demography, black circles show the original test and coloured circles show the test adjusted to the maximum likelihood demographics (for a given number of SNPs). Results of the estimation based on 10^4 SNPs are shown in panel a, and on 10^5 SNPs in panel b. (c)-(d) Same as in panels a, b, respectively, but for demographic histories shown in Fig. 3d. Scaled mutation rate used: $\theta = 100$. Number of independent gene genealogies simulated: 10^6 .

circles). For comparison, we also show the distributions of Tajima's D adjusted to the corresponding actual demographics (grey regions), and to the constant population-size history, i. e. original Tajima's D (black circles). Fig. 4a and b show the results based on 10^4 SNPs, and Fig. 4c and d show the results based on 10^5 SNPs. Our results show that Tajima's D adjusted to the ML-demography coincides well with Tajima's D adjusted to the actual underlying history if the demography estimation is performed using $\geq 10^5$ SNPs (compare Fig. 4a and c to Fig. 4b and d). Note, that while we adjust the tests for the first two moments, demography influences also higher moments. This leads to a skewness of the adjusted distributions versus the neutral ones as noticed already by Zivkovic and Wiehe (2008).

B. Estimated human demographics

We now analyze the reliability of the obtained frequency spectra of the human populations. Table II gives an overview of the variation contained in the empirical FSFSs of the populations. We focus on singletons (mutations of size 1) since they represent the most distinctive part of the frequency spectrum between populations. For each population we compare multiple SNP samplings of the same subsample of 30 individuals to those of different subsamples of the same size. It can be seen that our procedure to extract 10^5 SNPs essentially grasps the information contained in a specific subsample, since we find only minor changes by repeating it on the same sample. The variation between different subsamples, which is highest for LWK, may hint at some substructure in a given population. The populations CHB, CHS, GBR and CEU are not distinguishable by their amount of singletons (see Table II), but they become distinguishable when doubletons are taken into account (not shown). The difference between CHB and CHS remains small, though, and their whole frequency spectra are the most similar ones among all populations.

Our demography estimation shows (see Fig. 5 and Table S1 in Supplementary material) that the FSFSs of the non-African populations are consistent with a population bottleneck. By contrast, the FSFS of the African population ASW is consistent with two population-size expansions, and the FSFSs of LWK and YRI are consistent with an inverse bottleneck.

C. Neutrality tests adjusted to the estimated human demographics

Figure 6 shows the original test values of Tajima's D plotted against the adjusted ones for nonoverlapping windows of size 100kb. The inclusion of demography into the tests basically results in an affine linear transformation of the test values (coefficient

TABLE II Average and standard deviation (SD) of singletons as an indicator of the differences between frequency spectra. Compared are four independent drawings of SNPs (each 10^5 SNPs) out of the same population subsample with those of different subsamples. A subsample consists of 30 individuals.

Population	Intra-sample average	SD	Inter-sample average	SD
CEU	2029	14.0	2043	25.0
FIN	1894	16.9	1896	18.9
GBR	2062	9.4	2064	17.1
TSI	2165	9.5	2165	9.2
CHB	2039	16.2	2031	23.9
CHS	2048	13.3	2036	52.2
JPT	1955	10.8	1944	16.7
ASW	2837	7.3	2833	23.0
LWK	2665	15.3	2652	71.6
YRI	2352	6.6	2350	24.4

of determination $R^2 \approx 0.99$). Since θ is large ($\theta > 50$ for almost all regions), this observation fits our theoretical result of Eq. (7). The residuals of a linear regression of the adjusted on the original values are approximately normally distributed with standard deviation of ≈ 0.07 . This suggests that the scattering observed in the figure should be interpreted as noise and not as a biological phenomenon. Some of the “outliers” appear to be due to windows containing very few SNPs. However, on the other hand, we notice that the residuals of different subsamples are correlated ($R^2 \geq 0.5$) for the same population, but not for different populations. This hints at a possible systematic effect. The linearity implies that the empirical quantiles of the test statistics are unaffected by the adjustment.

D. Identifying candidate regions of positive selection

We compare Tajima’s D between the four subsamples of the same population. The coefficient of determination is about $R^2 \approx 0.8$ in all populations. The highest correlation between samples from different populations show CHB with CHS ($R^2 \approx 0.73$), and CEU with GBR ($R^2 \approx 0.71$). The lowest correlation show LWK or YRI compared with the Asian populations ($R^2 \approx 0.1$). We find that CRTRs vary considerably among subsamples of the same population. We therefore add a condition and require the test statistic of a particular window to be in the 1%-quantile simultaneously for all four subsamples. From these windows we construct CRTRs as described above. The additional constraint reduces the number of CRTRs by more than 50%. For the populations CEU, CHB and YRI the obtained regions are depicted in Figure 7. We obtain 7 (10 for adjusted test values) CRTRs for population CEU, 10 (11) for CHB and 8 (6) for YRI, respectively. Carlson et al. (2005), using the SNP array data available at that time, obtained 7 CRTRs for the African, 23 for the European and 29 for the Chinese population samples which only partially overlap with ours. These differences are caused most likely by the distinct population samples used. In the supplement we list CRTRs of all 10 populations. If the relation between original and adjusted test values was linear, their respectively detected regions should be identical. The observed differences are probably due to noise which, even if small, leads to split or fused CRTRs.

IV. DISCUSSION AND CONCLUSIONS

The aim of this study was to incorporate the effects of varying population sizes into SFS-based tests of the neutral evolution hypothesis. We achieved this by adjusting the first two moments of the site frequency spectrum (SFS) to correspond to a given demography. For populations of constant size the ‘adjusted’ tests are identical to the original ones. Our procedure generalises previous results regarding demography-adjustment of Tajima’s D (Zivkovic and Wiehe, 2008).

When dealing with experimental data, the demography used for adjusting the tests needs to be either known from other sources or to be estimated. One method for the estimation is the ML-procedure applied to single nucleotide polymorphisms (SNPs) sampled at physically distant sites, as proposed by Nielsen (2000) (see also Adams and Hudson (2004)). Under this method, individual SNPs are independent from each other and therefore the corresponding SFS counts are multinomially distributed, which simplifies mathematical treatment. Since the parameters of the estimated demography usually differ from those of the real (but generally unknown) demography, we tested by means of computer simulations how sensitive ML-estimates are with respect to the number of SNPs used for estimation. We fitted folded site frequency spectra (FSFSs) simulated under two

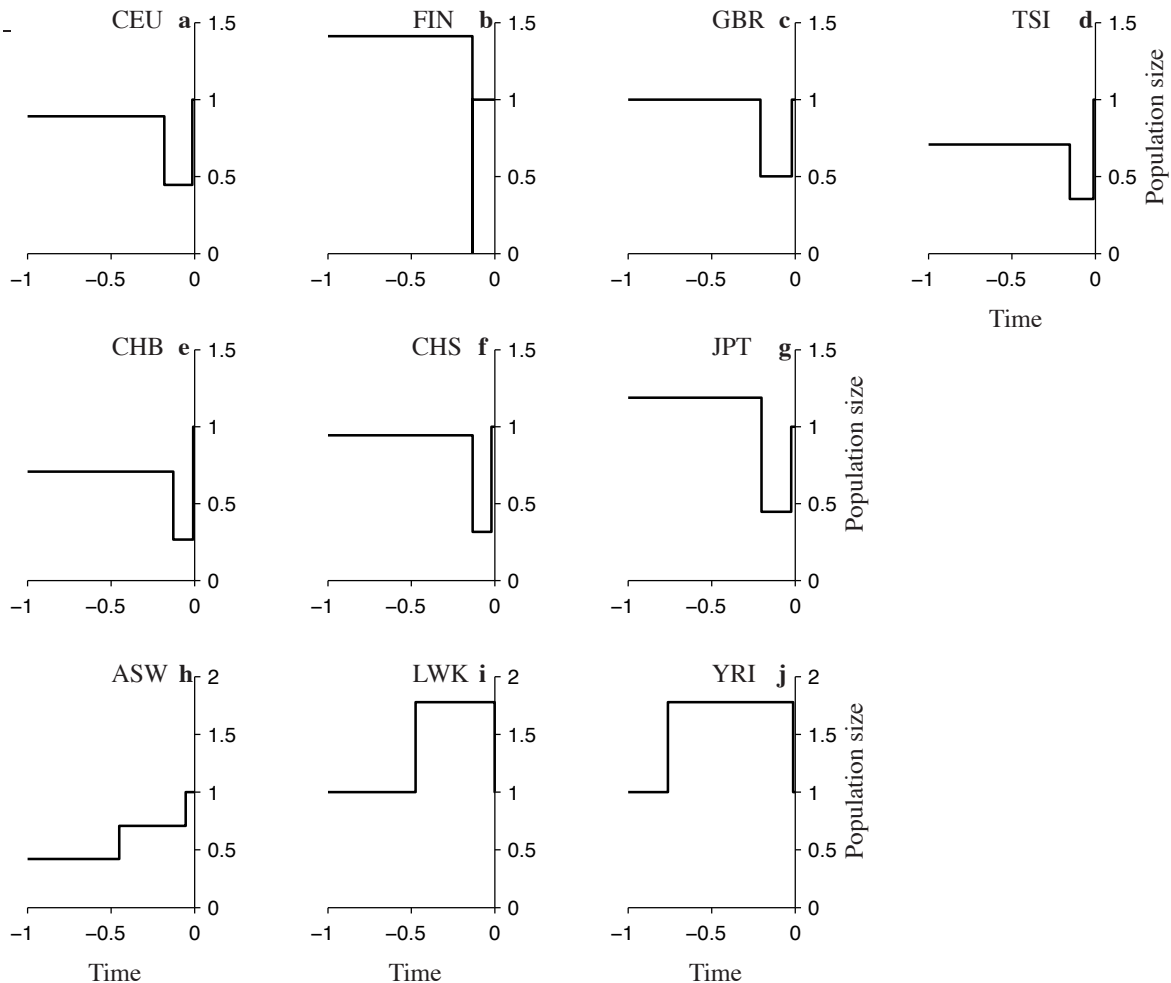


FIG. 5 Estimated demographies for 10 human populations. Note that the demographies of LWK and YRI have identical shape (inverse bottleneck). However, in both cases the population-size decline is so recent, that it cannot be seen on this scale. In each panel, the size is scaled by N_1 , and time is scaled by $2N_1$.

reference demographies, one being a recent bottleneck, and the other being a past population-size expansion followed by a recent decline. These two demographies are instances of a demographic model with two population-size changes in the past. Such a model is believed to capture the essence (Adams and Hudson, 2004; Marth et al., 2004; Stajich and Hahn, 2005) of the out-of-Africa expansion of humans (Cavalli-Sforza and Feldman, 2003; Eriksson et al., 2012; Liu et al., 2006; Ramachandran et al., 2005; Tanabe et al., 2010). Despite its simplicity four parameters have to be estimated, and therefore a large number of parameter combinations to be tested. However, it yields exact analytical expressions for the first two moments of the SFS by combining the results of Fu (1995) with those of Eriksson et al. (2010). Note that these expressions are also helpful to find optimal tests of neutrality under piecewise constant demographies (Ferretti et al., 2010). As expected, we found that ML estimation of demography is consistent: the estimated parameters converge to those of the true demography with increasing number of SNPs. The spectrum corresponding to the ML-demography is almost indistinguishable from the spectrum corresponding to the real underlying demography if the estimation is based on more than 100,000 SNPs. We confirmed this finding for our two reference demographies by comparing Tajima's D adjusted to the actual underlying demography, with that adjusted to the ML-demography.

After confirming the validity of the ML-procedure, we applied our method to disentangle the effects of selection and demography using data from the 1000 genomes project (McVean et al., 2012). We sampled the FSFSs of ten human populations from physically distant intergenic regions (presumably neutral (Adams and Hudson, 2004)) in order to estimate the ML-parameters of the piecewise constant demographic model with two population-size changes in the past allowing for population size parameter changes of at most two orders of magnitude (Marth et al., 2004). The time parameters were allowed to vary by three orders of magnitude (i.e. from -3 to 0 on logarithmic scale). The lower boundary for the times corresponds to only 10 generations (that

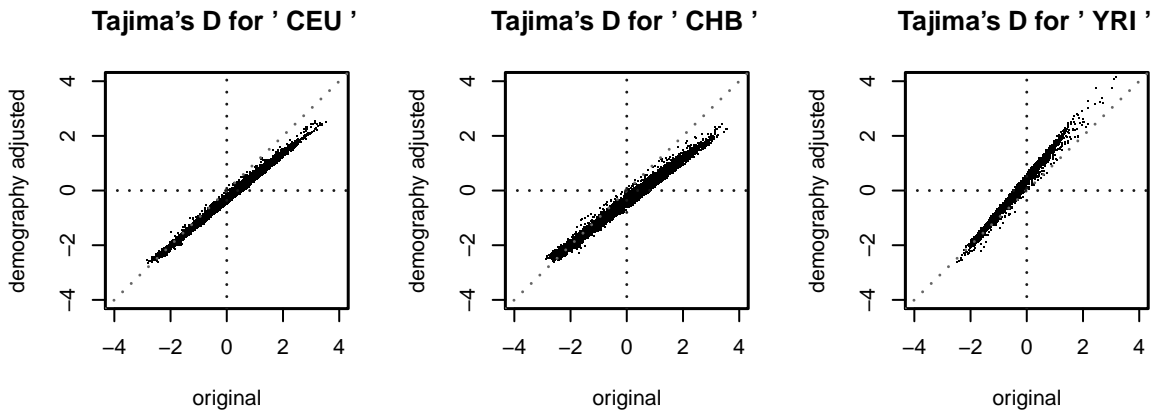


FIG. 6 Scatterplots of original vs adjusted tests, for non-overlapping windows; ≈ 26500 data points. Fraction of variance explained $R^2 \approx 0.98$ in all three cases.

is, 200 – 250 years, under the assumption that a human generation time is 20 – 25 years (Marth et al., 2004)). This is a very short time, and we do not expect that demographic changes occurring on even shorter timescales would be detected by the site frequency spectra (since the process of mutations is slow). In fact, Eq. (13) in Appendix IV shows that in the limit $t_1 \rightarrow 0$, the SFS, and therefore the FSFS, corresponds to that of a two-stage demography with population size equal to x_2 in the first stage, and x_3 in the second stage. The upper boundary for the times was chosen to coincide with the emergence of anatomically modern humans about 200,000 years ago (see Cavalli-Sforza and Feldman (2003) and references therein).

Our results are mainly consistent with the results of Adams and Hudson (2004) and on Marth et al. (2004): the ML-demographies of non-African populations correspond to a bottleneck, and the ML-demography of one of the sampled African populations (ASW) corresponds to two subsequent population-size expansions. The FSFSs of the remaining two African populations (LWK and YRI) gave rise to demographies with a distant population-size expansion followed by a population-size decline.

In order to detect regions under selection, we computed genome-wide values of three tests of neutrality, by scanning over sliding windows with 100 kb, as proposed by Carlson et al. (2005). We find that the distributions of the adjusted tests are very similar to each other, suggesting that the differences between the original distributions can be explained to a large part by demography. We find that the adjusted test values are essentially affine linear transformations of the original ones. This leads to largely identical quantiles and, consequently, identical candidate regions for selection. Our results show that it is valid to use the original tests in order to detect selection as long as the empirical distribution of test values of the whole genome is used as reference. The adjusted values are however useful, as they facilitate direct comparisons of test values from different populations. Therefore we provide our genome scans of both original and adjusted tests as tracks for the UCSC genome browser.

Carlson et al. (2005) calculated the correlation between Tajima's D derived from SNP array data with that from resequenced genes from the same individuals. We compare the former with our values for all windows and find a lower correlation, most likely due to distinct population samples. As a consequence, also the candidate regions of selection show only modest overlap. We find that the specification of these regions as long consecutive stretches of extremely low Tajima's D , while in general useful, is sensitive to minor changes in single windows. We therefore try to make this concept more robust by requiring windows to belong to the respective lower 1%-quantile in several subsamples of the same population. This reduces drastically the amount of candidate regions. The differences between regions identified using original vs adjusted values is the result of the slight scattering of the transformation which splits some contiguous regions and fuses others.

Concerning the validity and consistency of our results, our main point is that the inference of demography by the ML-approach is very sensitive to minor changes in the frequency spectrum. Myers et al. (2008) even stated, that the (theoretical) existence of very different demographies with exactly the same frequency spectrum precludes such an inference altogether. Our results do not support this overly pessimistic view. Rather, we find that ML-parameter estimation of an, admittedly, simple demographic model is consistent.

We emphasize, that the adjustment of the tests relies on the absolute values of the inferred moments (ξ_i^0 and σ_{ij}^0) which are a function of the entire demography not just of quantities (e.g. θ) at present time. In particular, we observe, that different demographies with similar frequency spectrum can in principle lead to different variances of the adjusted tests.

As is common practise, we ignored recombination, although it is known that recombination reduces the variance of the tests considered. Since recombination is not uniform across the genome, neglecting it causes a distortion of the test distributions.

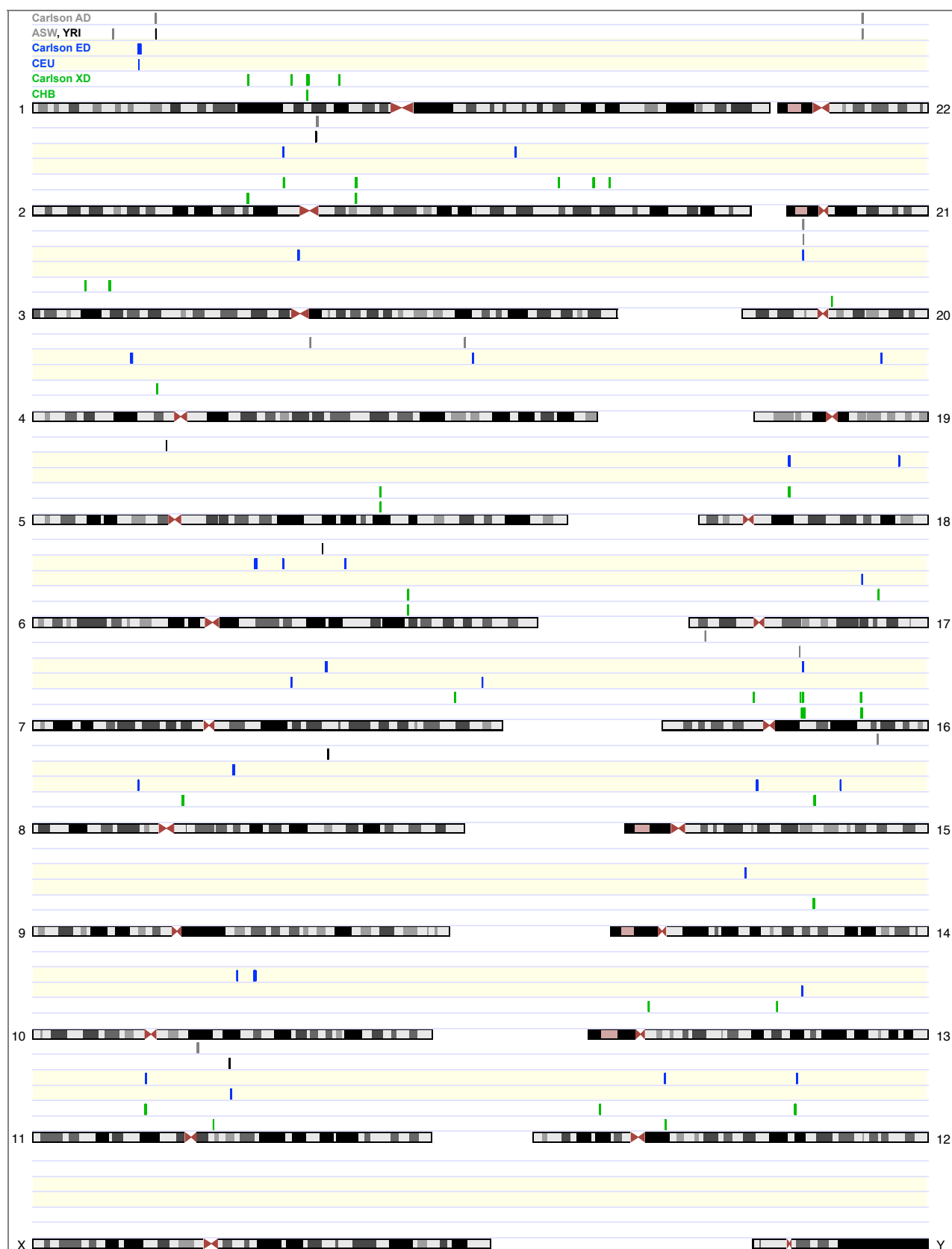


FIG. 7 Contiguous regions of Tajima's D reduction ("CRTR") from Carlson et al. (2005) compared with those derived from our demography-adjusted test. From above to beneath: Carlson: African descent (gray); ASW (gray) and YRI (black); Carlson: European-descent (blue); CEU; Carlson: Chinese-descent (green); CHB. The regions found by Carlson et al. have been translated from hg17 to hg19 coordinates.

However, the demography-adjusted tests studied here serve as a basis for further work in which recombination and rate inhomogeneity across genomes is taken into account.

The program used to calculate the adjusted test statistics is available as C++ source code on <http://ntx.sourceforge.net/> and tracks for the UCSC browser containing test values (original as well as adjusted) for all ten populations are available at <http://jakob.genetik.uni-koeln.de/data/>.

Acknowledgements. This work was financially supported by grants from Vetenskapsrådet, from the Göran Gustafsson Foundation for Research in Natural Sciences and Medicine, through the platform “Centre for Theoretical Biology” and from CeMEB at the University of Gothenburg to BM, and by a grant of the German Science Foundation (DFG-SFB680) to TW.

References

- Achaz, G., 2008. Testing for neutrality in samples with sequencing errors. *Genetics* 179 (3).
- Achaz, G., 2009. Frequency spectrum neutrality tests: One for all and all for one. *Genetics* 183 (1), 249–258.
- Adams, A. A., Hudson, R. R., 2004. Maximum-likelihood estimation of demographic parameters using the frequency spectrum of unlinked single-nucleotide polymorphisms. *Genetics* 168, 1699–1712.
- Akey, J. M., Eberle, M. A., Rieder, M. J., Carlson, C. S., Shriver, M. D., Nickerson, D. A., Kruglyak, L., 2004. Population history and natural selection shape patterns of genetic variation in 132 genes. *PLoS Biology* 2 (10), e286.
- Carlson, C. S., Thomas, D. J., Eberle, M. A., Swanson, J. E., Livingston, R. J., Rieder, M. J., Nickerson, D. A., 2005. Genomic regions exhibiting positive selection identified from dense genotype data. *Genome Research* 15, 1553–1565.
- Cavalli-Sforza, L. L., Feldman, M. W., 2003. The application of molecular genetic approaches to the study of human evolution. *Nature Genetics Supplement* 33, 266–275.
- Eriksson, A., Betti, L., Friend, A. D., Lycett, S. J., Singarayer, J. S., von Cramon-Taubadel, N., Valdes, P. J., Balloux, F., Manica, A., 2012. Late Pleistocene climate change and the global expansion of anatomically modern humans. *Proceedings of the National Academy of Sciences* 110 (40), 16089–16094.
- Eriksson, A., Mehlig, B., Rafajlovic, M., Sagitov, S., 2010. The total branch length of sample genealogies in populations of variable size. *Genetics* 186 (2), 601–611.
- Fay, J. C., Wu, C.-I., 2000. Hitchhiking under positive Darwinian selection. *Genetics* 155 (3), 1405–1413.
- Ferretti, L., Perez-Enciso, M., Ramos-Onsins, S., 2010. Optimal neutrality tests based on the frequency spectrum. *Genetics* 186 (1), 353–365.
- Fisher, R. A., 1930. *The genetical theory of natural selection*. Clarendon, Oxford.
- Fu, Y. X., 1995. Statistical properties of segregating sites. *Theoretical Population Biology* 48 (2), 172 – 197.
- Fu, Y.-X., Li, W.-H., 1993a. Maximum likelihood estimation of population parameters. *Genetics* 134 (4), 1261–70.
- Fu, Y. X., Li, W. H., 1993b. Statistical tests of neutrality of mutations. *Genetics* 133 (3), 693–709.
- Kingman, J. F. C., 1982. The coalescent. *Stochastic Processes and their Applications* 13 (3), 235 – 248.
- Liu, H., Prugnolle, F., Manica, A., Balloux, F., 2006. A geographically explicit genetic model of worldwide human-settlement history. *Am. J. Hum. Genet.* 79 (2), 230–237.
- Marth, G. T., Czabarka, E., Murvai, J., Sherry, S. T., 2004. The allele frequency spectrum in genome-wide human variation data reveals signals of differential demographic history in three large world populations. *Genetics* 166 (1), 351–372.
- McVean, et al., 2012. An integrated map of genetic variation from 1092 human genomes. *Nature* 491, 56–65.
- Myers, S., Fefferman, C., Patterson, N., 2008. Can one learn history from the allelic spectrum? *Theoretical Population Biology* 73, 342–348.
- Nielsen, R., 2000. Estimation of population parameters and recombination rates from single nucleotide polymorphisms. *Genetics* 154, 931–942.
- Nielsen, R., Bustamante, C., Clark, A. G., Glanowski, S., Sackton, T. B., Hubisz, M. J., Fledel-Alon, A., Tanenbaum, D. M., Civello, D., White, T. J., J. Sninsky, J., Adams, M. D., Cargill, M., 2005. A scan for positively selected genes in the genomes of humans and chimpanzees. *PLoS Biol* 3 (6), e170.
- Ramachandran, S., Deshpande, O., Roseman, C., Rosenberg, N., Feldman, M., Cavalli-Sforza, L., 2005. Support from the relationship of genetic and geographic distance in human populations for a serial founder effect originating in Africa. *Proceedings of the National Academy of Sciences of the United States of America* 102 (44), 15942–15947.
- Stajich, J. E., Hahn, M. W., 2005. Disentangling the effects of demography and selection in human history. *Mol. Biol. Evol.* 22 (1), 63–73.
- Tajima, F., 1989a. Statistical method for testing the neutral mutation hypothesis by DNA polymorphism. *Genetics* 123 (3), 585–595.
- Tanabe, K., Mita, T., Jombart, T., Eriksson, A., Horibe, S., Palacpac, N., Ranford-Cartwright, L., Sawai, H., Sakihama, N., Ohmae, H., Nakamura, M., Ferreira, M. U., Escalante, A. A., Prugnolle, F., Björkman, A., Färnert, A., Kaneko, A., Horii, T., Manica, A., Kishino, H., Balloux, F., 2010. Plasmodium falciparum accompanied the human expansion out of Africa. *Curr Biol* 20 (14), 1283–1289.
- Tang, K., Thornton, K. R., Stoneking, M., 2007. A new approach for using genome scans to detect recent positive selection in the human genome. *PLoS Biol* 5 (7), e171.
- Voight, B. F., Kudaravalli, S., Wen, X., Pritchard, J. K., 2006. A map of recent positive selection in the human genome. *PLoS Biol* 4 (3), e72.
- Wright, S., 1931. Evolution in mendelian populations. *Genetics* 16, 97–159.
- Zeng, K., Fu, Y.-X., Shi, S., Wu, C.-I., 2006. Statistical tests for detecting positive selection by utilizing high-frequency variants. *Genetics* 174, 1431–1439.
- Zivkovic, D., Wiehe, T., 2008. Second-order moments of segregating sites under variable population size. *Genetics* 180 (1), 341–357.

Appendix A: The denominator of demography-adjusted tests of neutrality based on the SFS

As explained in Section II, all tests of neutrality based on the SFS can be expressed using a general form, Eq. (2). The numerator of Eq. (2) depends on the first moment of the SFS under a given demography. Similarly, the denominator of Eq. (2) depends on the second moment of the SFS under a given demography. We find:

$$\begin{aligned}
\text{Var}\left[\sum_{i=1}^{n-1} \Omega_i \hat{\theta}^{(i)}\right] &= \text{Var}\left[\sum_{i=1}^{n-1} \Omega_i \frac{\xi_i}{\xi_i^0}\right] \\
&= \sum_{i=1}^{n-1} \text{Var}\left(\Omega_i \frac{\xi_i}{\xi_i^0}\right) + \sum_{\substack{i,j=1 \\ i \neq j}}^{n-1} \text{Cov}\left(\Omega_i \frac{\xi_i}{\xi_i^0}, \Omega_j \frac{\xi_j}{\xi_j^0}\right) \\
&= \sum_{i=1}^{n-1} \left(\frac{\Omega_i}{\xi_i^0}\right)^2 \text{Var}(\xi_i) + \sum_{\substack{i,j=1 \\ i \neq j}}^{n-1} \frac{\Omega_i}{\xi_i^0} \text{Cov}(\xi_i, \xi_j) \frac{\Omega_j}{\xi_j^0} \\
&= \theta \sum_{i=1}^{n-1} \Omega_i^2 \frac{1}{\xi_i^0} + \theta^2 \sum_{i=1}^{n-1} \left(\frac{\Omega_i}{\xi_i^0}\right)^2 \sigma_{ii}^0 + \theta^2 \sum_{\substack{i,j=1 \\ i \neq j}}^{n-1} \frac{\Omega_i}{\xi_i^0} \sigma_{ij}^0 \frac{\Omega_j}{\xi_j^0} \\
&= \theta \sum_{i=1}^{n-1} \Omega_i^2 \frac{1}{\xi_i^0} + \theta^2 \sum_{i,j=1}^{n-1} \frac{\Omega_i}{\xi_i^0} \sigma_{ij}^0 \frac{\Omega_j}{\xi_j^0}
\end{aligned} \tag{10}$$

Here one has $\sigma_{ij}^0 = \text{Cov}(\xi_i, \xi_j)|_{\theta=1}$, for $i \neq j$, and $\sigma_{ii}^0 = (\text{Var}(\xi_i) - \langle \xi_i \rangle)|_{\theta=1}$. Eq. (10) corresponds to Eq. (3) given in the main text. Note that for the constant population size one has $\xi_i^0 = 1/i$, and σ_{ij}^0 is given by Fu (1995). Thus, Eq. (10) reduces to Eq. (9) in Achaz (2009).

In order to compute Eq. (10) using the observed spectrum, one needs to have an estimate of θ^2 . For a given estimator of θ , that is based on weights $\omega_1, \dots, \omega_{n-1}$, i.e. $\hat{\theta}_\omega = \sum_{i=1}^{n-1} \omega_i \xi_i / \xi_i^0$, it holds

$$\langle \hat{\theta}_\omega^2 \rangle = \text{Var}[\hat{\theta}_\omega] + \langle \hat{\theta}_\omega \rangle^2 = \theta \sum_{i=1}^{n-1} \frac{\omega_i^2}{\xi_i^0} + \theta^2 \sum_{i,j=1}^{n-1} \frac{\omega_i}{\xi_i^0} \sigma_{ij}^0 \frac{\omega_j}{\xi_j^0} + \theta^2 = y_n \theta + (1 + z_n) \theta^2,$$

with

$$y_n = \sum_{i=1}^{n-1} \frac{\omega_i^2}{\xi_i^0} \text{ and } z_n = \sum_{i,j=1}^{n-1} \frac{\omega_i}{\xi_i^0} \sigma_{ij}^0 \frac{\omega_j}{\xi_j^0}. \tag{11}$$

It follows that

$$\langle \hat{\theta}_\omega^2 \rangle - y_n \langle \hat{\theta}_\omega \rangle = \theta^2 (1 + z_n).$$

Solving the latter with respect to θ^2 yields:

$$\theta^2 = \frac{\langle \hat{\theta}_\omega^2 \rangle - y_n \langle \hat{\theta}_\omega \rangle}{1 + z_n}.$$

Hence, as an estimator for θ^2 we take

$$\widehat{\theta}_\omega^2 = \frac{\hat{\theta}_\omega^2 - y_n \hat{\theta}_\omega}{1 + z_n}. \tag{12}$$

This expression corresponds to Eq. (4) given in the main text.

Appendix B: The first two moments of the SFS

In this appendix we compute the first two moments of the SFS, $\langle \xi_i \rangle$ and $\langle \xi_i \xi_j \rangle$, under a varying population size. We consider a large, well mixed, randomly mating diploid Wright-Fisher population with a varying population size. We assume that mutations accumulate according to the infinite sites model at rate μ per generation per site. The scaled mutation rate, θ , per genetic sequence of length L is given by $\theta = 4\mu N_1 L$, where N_1 denotes the present population size. We consider the SFS corresponding to gene genealogies of n individuals. The scaled time during which gene genealogies have exactly $k \leq n$ lines is denoted by τ_k below (i. e. τ_k stands for $\lfloor 2N_1 \tau_k \rfloor$ generations).

The first two moments of the SFS can be expressed as (Fu, 1995)

$$\langle \xi_i \rangle = \frac{\theta}{2} \sum_{k=2}^n k p(k, i) \langle \tau_k \rangle, \quad (13)$$

$$\begin{aligned} \langle \xi_i \xi_j \rangle = & \delta_{i,j} \sum_{k=2}^n k p(k, i) \left(\frac{\theta}{2} \langle \tau_k \rangle + \frac{\theta^2}{4} \langle \tau_k^2 \rangle \right) \\ & + \frac{\theta^2}{4} \left\{ \sum_{k=2}^n k(k-1) p(k, i; k, j) \langle \tau_k^2 \rangle + \sum_{k < m} k m (p(k, i; m, j) + p(k, j; m, i)) \langle \tau_k \tau_m \rangle \right\}. \end{aligned} \quad (14)$$

where

$$\delta_{i,j} = \begin{cases} 1, & \text{for } i = j, \\ 0, & \text{for } i \neq j, \end{cases} \quad (15)$$

$$p(k, i) = \frac{\binom{n-k}{i-1} k - 1}{\binom{n-1}{i} i}, \quad (16)$$

$$p(k, i; k, j) = \begin{cases} \frac{\binom{n-i-j-1}{k-3}}{\binom{n-1}{k-1}}, & \text{for } k > 2, \\ p(k, i), & \text{for } k = 2, \text{ and } i + j = n, \\ 0, & \text{for } k = 2, \text{ and } i + j \neq n, \end{cases} \quad (17)$$

$$p(k, i; m, j) = (\delta_{\lfloor i/j \rfloor, 0} + \delta_{i,j}) p_a(k, i; m, j) + (\delta_{\lfloor (i+j)/n \rfloor, 0} + \delta_{i+j, n}) p_b(k, i; m, j). \quad (18)$$

The probabilities $p_a(k, i; m, j)$, and $p_b(k, i; m, j)$ in Eq. (18) are (Fu, 1995)

$$p_a(k, i; m, j) = \begin{cases} \sum_{t=2}^{\min(m-k+1, i-j+1)} \frac{\binom{m-k}{t-1} k-1}{\binom{m-1}{t} m} \frac{\binom{i-j-1}{t-2} \binom{n-i-1}{m-t-1}}{\binom{n-1}{m-1}}, & \text{for } j < i \\ \frac{k-1}{m(m-1)} \frac{\binom{n-i-1}{m-2}}{\binom{n-1}{m-1}}, & \text{for } i = j, \end{cases} \quad (19)$$

$$p_b(k, i; m, j) = \begin{cases} \sum_{t=1}^{\min(m-2, m-k+1, i)} \frac{\binom{m-k}{t-1} (k-1)(m-t)}{\binom{m-1}{t} t m} \frac{\binom{i-1}{t-1} \binom{n-i-j-1}{m-t-2}}{\binom{n-1}{m-1}}, & \text{for } k > 2 \\ \frac{1}{j m} \frac{\binom{n-m}{j-1}}{\binom{n-1}{j}}, & \text{for } k = 2, \text{ and } i + j = n. \end{cases} \quad (20)$$

In the limit $\theta \rightarrow 0$, Eq. (14) reduces to:

$$\langle \xi_i^2 \rangle = \frac{\theta}{2} \langle \xi_i \rangle, \text{ and } \langle \xi_i \xi_{j \neq i} \rangle = 0 \text{ for } \theta \rightarrow 0. \quad (21)$$

In other words, in this limit the SFS counts are multinomially distributed, as explained in Section II.

For constant population size, it follows from Eq. (13) that $i \langle \xi_i \rangle = \theta$, independently of i . By contrast, for demographic history shown in Fig. 2, this is not true. Using the results of Eriksson et al. (2010), in this case we find:

$$\langle \xi_i \rangle = \frac{\theta}{2} \sum_{m_1=2}^n a_{m_1}^{(ni)} f_{m_1}, \text{ for } i = 1, \dots, n-1, \quad (22)$$

where $a_{m_1}^{(ni)}$, and f_{m_1} are:

$$a_{m_1}^{(ni)} = \sum_{k=2}^{m_1} k c_{nkm_1} p(k, i), \quad (23)$$

$$f_{m_1} = b_{m_1}^{-1} \left(1 - (1 - x_2) e^{-b_{m_1} t_1} + (x_3 - x_2) e^{-b_{m_1} t_1} e^{-b_{m_1} s_2} \right). \quad (24)$$

Here, $x_2 = N_2/N_1$, $x_3 = N_3/N_1$, $s_2 = t_2/x_2$, $b_{m_1} = \binom{m_1}{2}$, and c_{nkm_1} is given by Eq. (11) in Eriksson et al. (2010). This result is consistent with Eq. (1) in Marth et al. (2004), assuming $M = 3$ in the model of Marth et al. (2004).

In what follows, we list our results for $\langle \xi_i \xi_j \rangle$ under the demographic history shown in Fig. 2. We find:

$$\langle \xi_i \xi_j \rangle = \delta_{i,j} \left(\langle \xi_i \rangle + \frac{\theta^2}{4} \sum_{m_1=2}^n \sum_{k=2}^{m_1} a_{m_1 k}^{(nij)} f_{m_1 k} \right) + \frac{\theta^2}{4} \sum_{m_1=2}^n \left(\sum_{k=2}^{m_1} g_{m_1 k}^{(nij)} f_{m_1 k} + \sum_{m_2=2}^{m_1} h_{m_1 m_2}^{(nij)} f_{m_1 m_2} \right), \quad (25)$$

where

$$a_{m_1 k}^{(nij)} = 2k c_{nkm_1} c_{kkk} p(k, i), \quad (26)$$

$$g_{m_1 k}^{(nij)} = 2k(k-1) c_{nkm_1} c_{kkk} p(k, i; k, j) \quad (27)$$

$$h_{m_1 m_2}^{(nij)} = \sum_{l=m_2}^{m_1} l c_{nlm_1} \sum_{k=2}^{m_2} k c_{lkm_2} [p(k, i; l, j) + p(k, j; l, i)]. \quad (28)$$

For the terms f_{m_1, m_2} in Eq. (25), we consider separately the cases $m_1 \neq m_2$, and $m_1 = m_2$. For the case $m_1 \neq m_2$, we find

$$\begin{aligned} f_{m_1 m_2} = & \\ & \frac{1}{b_{m_2}} \left\{ \frac{1 - e^{-b_{m_1} t_1} [1 - x_2^2 + (x_2^2 - x_3^2) e^{-b_{m_1} s_2}]}{b_{m_1}} \right. \\ & - [1 - x_2 + (x_2 - x_3) e^{-b_{m_2} s_2}] \frac{e^{-b_{m_2} t_1} - e^{-b_{m_1} t_1}}{b_{m_1} - b_{m_2}} \\ & \left. + x_2 (x_3 - x_2) e^{-b_{m_1} t_1} \frac{e^{-b_{m_2} s_2} - e^{-b_{m_1} s_2}}{b_{m_1} - b_{m_2}} \right\}. \quad (29) \end{aligned}$$

For the case $m_1 = m_2$, we obtain:

$$\begin{aligned} f_{m_1 m_1} = & \\ & \frac{1}{b_{m_1}} \left\{ \frac{1 - e^{-b_{m_1} t_1} [1 - x_2^2 + (x_2^2 - x_3^2) e^{-b_{m_1} s_2}]}{b_{m_1}} \right. \\ & - t [1 - x_2 + (x_2 - x_3) e^{-b_{m_2} s_2}] e^{-b_{m_1} t_1} \\ & \left. + x_2 (x_3 - x_2) s_2 e^{-b_{m_1} t_1} e^{-b_{m_1} s_2} \right\}. \quad (30) \end{aligned}$$

Eqs. (22)-(24) are used to find the demographic parameters that correspond to empirical data in terms of the maximum likelihood approach. Eqs. (25)-(30) are used to compute the tests of neutrality under the demographies found. The results are shown in Section III.

Supplementary Material

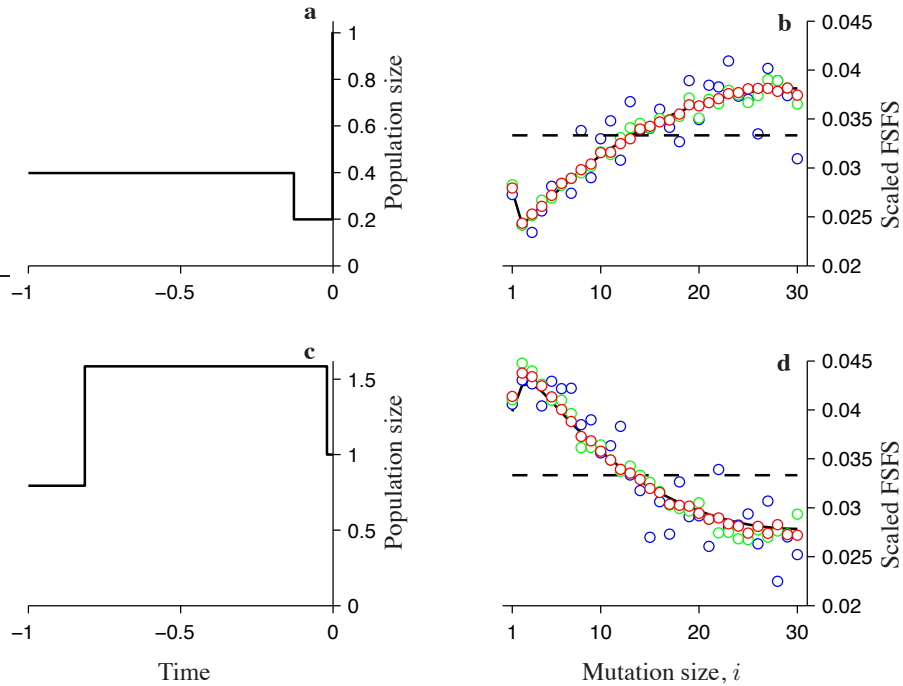


FIG. S1 (a), (c) Reference demographic histories (recent bottleneck in a, and a past population-size expansion followed by a recent decline in c). (b), (d) Scaled FSFSs computed analytically (black lines), together with the spectra obtained using our coalescent simulations containing 10^4 SNPs (blue circles), 10^5 SNPs (green circles) and 10^6 SNPs (red circles). Each spectrum is obtained by sampling one SNP from gene genealogies that have at least one mutation. The spectra are scaled so that in the constant population-size case, one obtains a constant equal to $1/\lfloor n/2 \rfloor$ (see dashed lines). Sample size: $n = 60$. Scaled mutation rate used: $\theta = 0.01$. Number of independent gene genealogies simulated: $2 \cdot 10^6$.

TABLE S1 Estimated demographic parameters using empirical spectra (the spectra are shown as black circles in Figs. S2-S4).

Population	$\log(t_1)$	$\log(t_2)$	$\log(x_2)$	$\log(x_3)$
CEU	-1.875	-0.775	-0.35	-0.05
FIN	-0.875	-2.975	-2	0.15
GBR	-1.7	-0.725	-0.3	0
TSI	-1.95	-0.85	-0.45	-0.15
CHB	-2.05	-0.925	-0.575	-0.15
CHS	-1.7	-0.95	-0.5	-0.025
JPT	-1.625	-0.75	-0.35	0.075
ASW	-1.275	-0.4	-0.15	-0.375
LWK	-3	-0.325	0.25	0
YRI	-1.925	-0.125	0.25	0

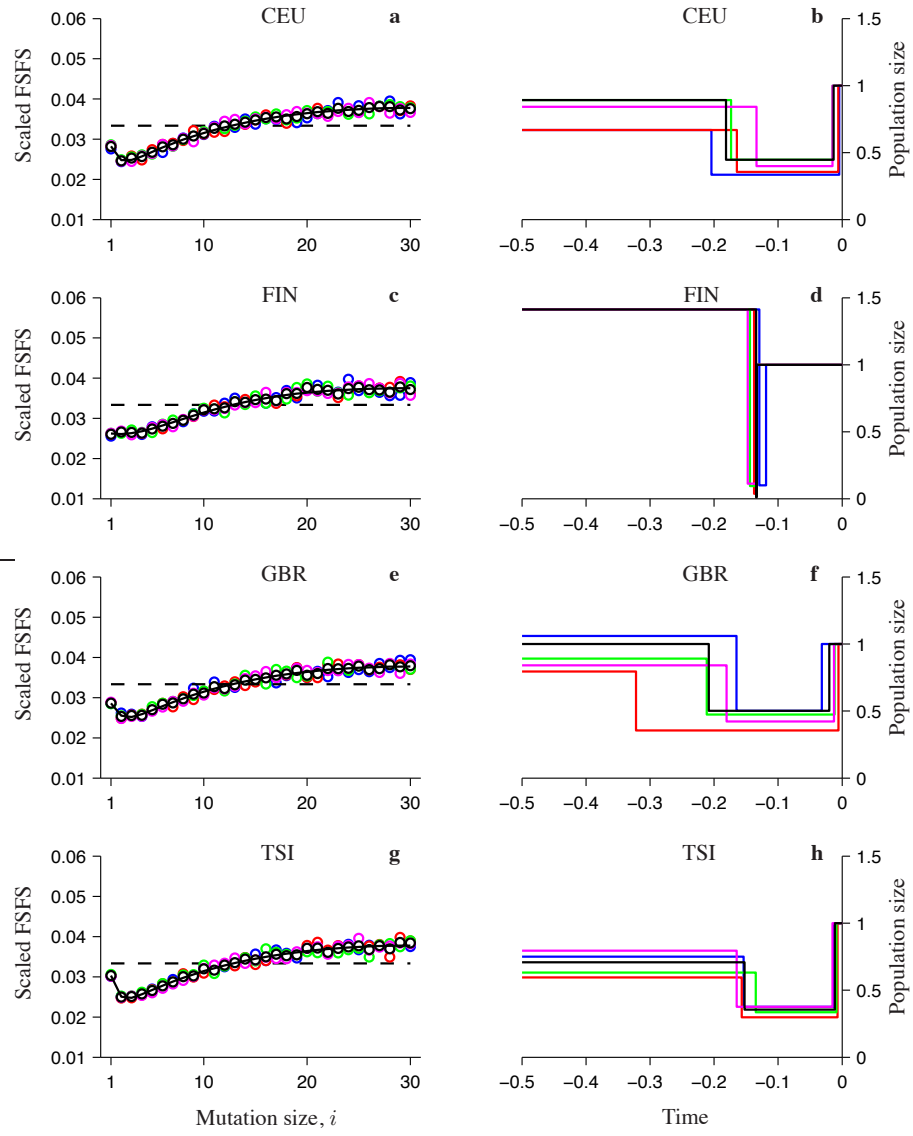


FIG. S2 (a), (c), (e), (g) Blue, red, green, and magenta circles show four empirically obtained scaled FSFSs for the four sampled European populations CEU (a), FIN (c), GBR (e), and TSI (g). The spectra are scaled so that in the constant population-size case one obtains a constant equal to $1/\lfloor n/2 \rfloor$ (shown by dashed lines). For each population black circles correspond to the spectrum obtained upon averaging over the forty sampled spectra. The corresponding best-fitted scaled spectra are shown by black lines. (b), (d), (f), (h) Best-fitted histories corresponding to the empirical spectra (demographies are coloured to match their fitted spectra).

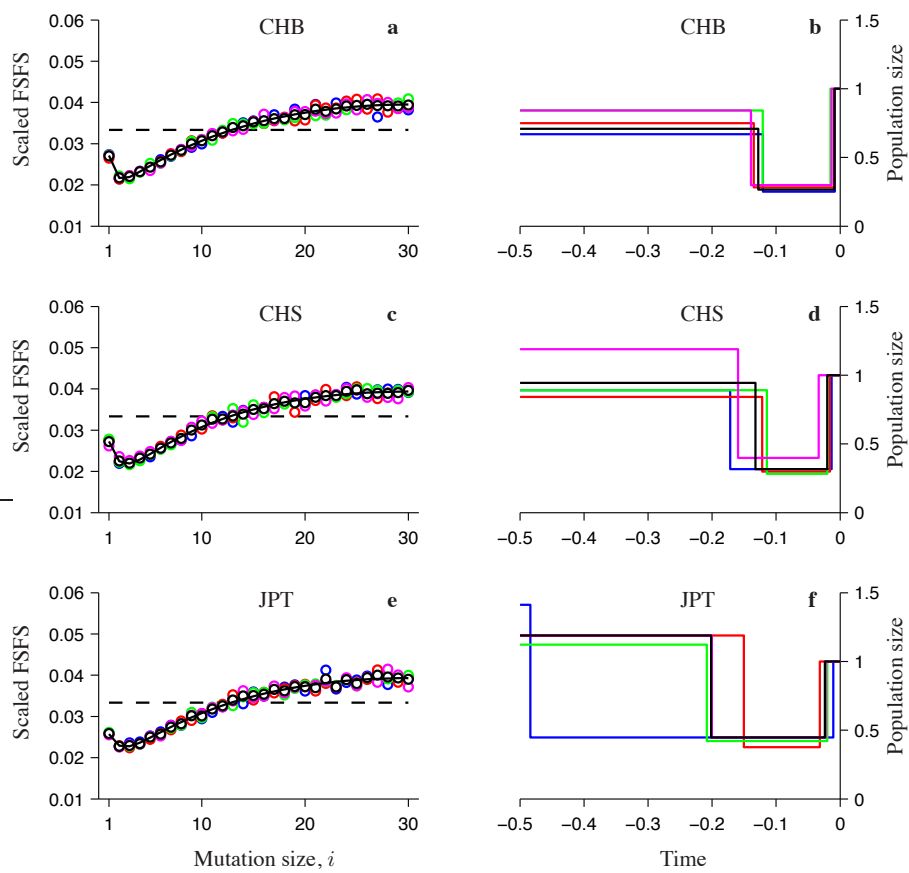


FIG. S3 Same as in Fig. S2 but for the populations with Asian ancestry.

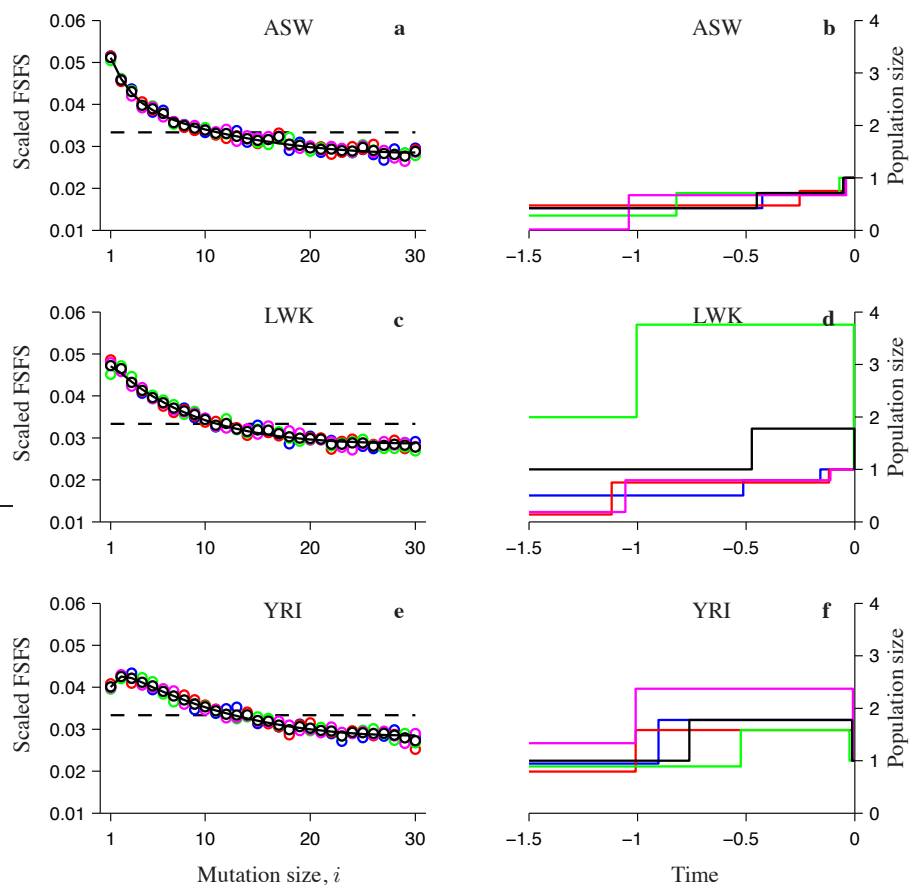


FIG. S4 Same as in Fig. S2 but for the populations with African ancestry.

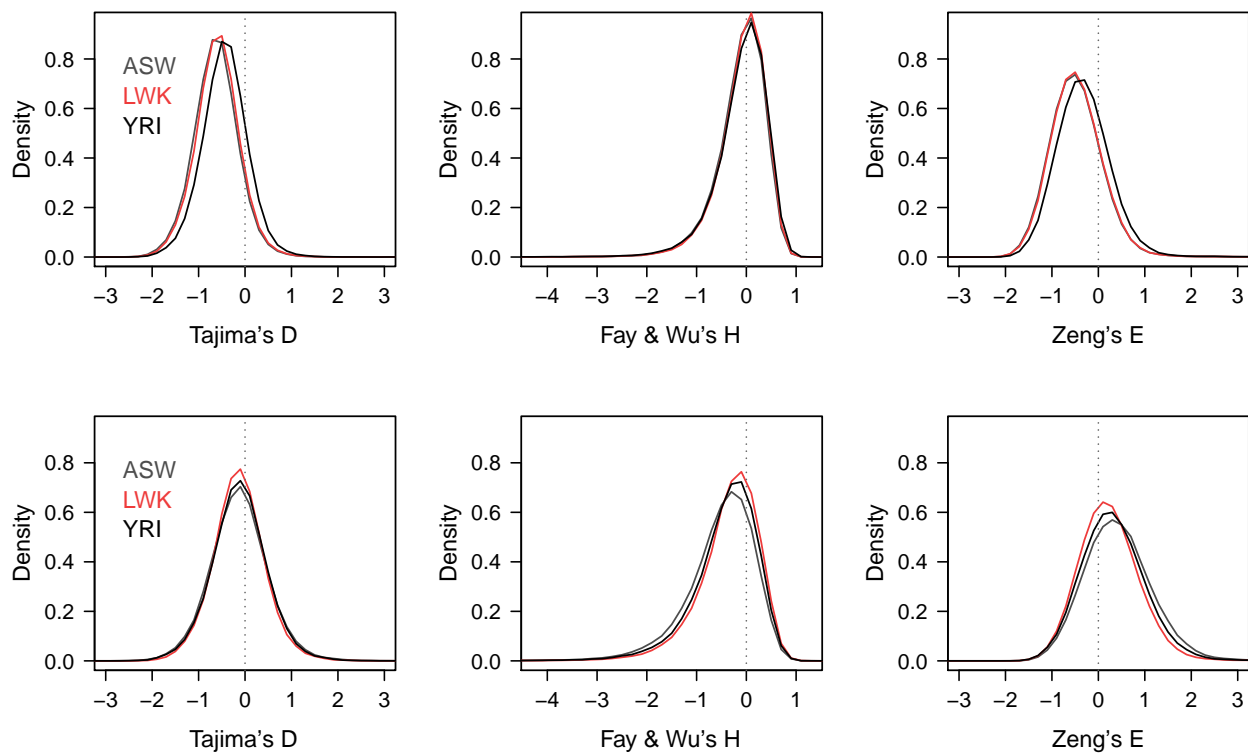


FIG. S5 Distribution of test values over all sliding windows. Top row: original tests. Bottom row: demography-adjusted tests.

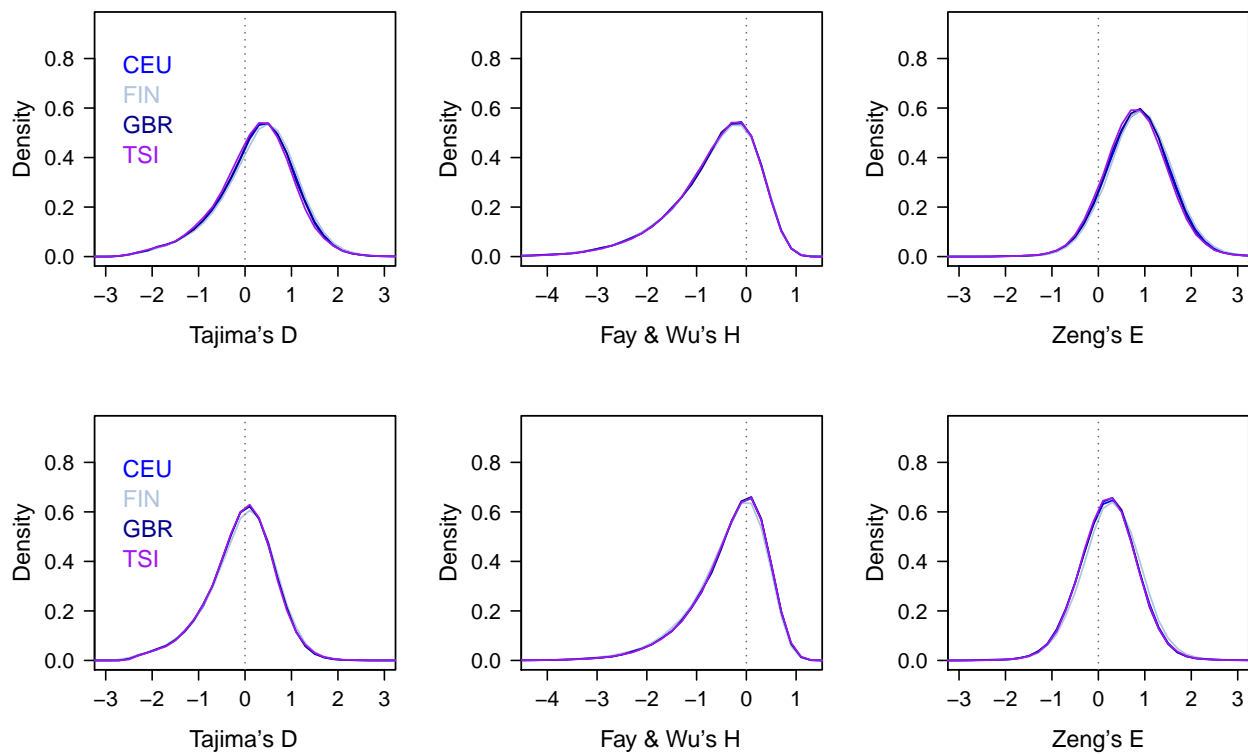


FIG. S6 Distribution of test values over all sliding windows. Top row: original tests. Bottom row: demography-adjusted tests.

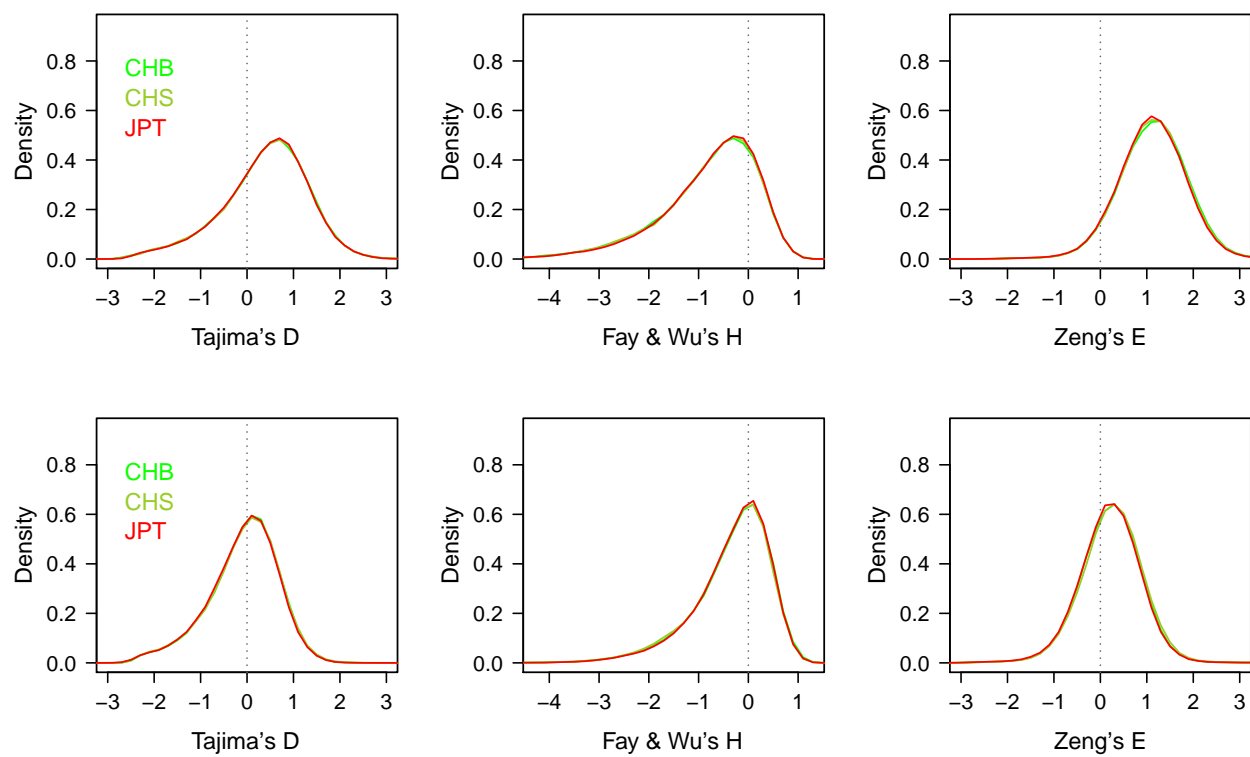


FIG. S7 Distribution of test values over all sliding windows. Top row: original tests. Bottom row: demography-adjusted tests.

Coordinates (hg19)		Windows	Known genes (UCSC)
ASW			
1	26.990.000	27.240.000	26 ARID1A, PIGV, ZDHHC18, SFN, GPN2, GPATCH3, NR0B2, BC016143
2	95.560.000	95.790.000	24 MAL, MRPS5
4	93.690.000	93.940.000	26 GRID2
4	145.890.000	146.130.000	25 ANAPC10, ABCE1, OTUD4, Mir_649
5	45.000.000	45.280.000	29 HCN1
5	133.980.000	134.190.000	22 SEC24A, CAMLG, DDX46, C5orf24
16	14.620.000	14.810.000	20 PARN, BFAR, PLA2G10, NPIP
16	46.470.000	46.660.000	20 ANKRD26P1, SHCBP1
20	20.460.000	20.740.000	29
22	28.400.000	28.790.000	40 Y_RNA
LWK			
1	41.500.000	41.710.000	22
2	95.560.000	95.760.000	21 MAL, MRPS5
2	96.790.000	96.990.000	21 DUSP2, CR749695, STARD7, LOC285033, TMEM127, CIAO1, SNRNP200
3	93.640.000	93.850.000	22 ARL13B, STX19, DHFRL1, NSUN3, U7
8	99.600.000	99.930.000	34
11	66.390.000	66.600.000	22 RBM14, RBM4, RBM4B, SPTBN2, C11orf80
17	44.210.000	44.400.000	20 LOC644246, ARL17A, LRRC37A
YRI			
1	41.500.000	41.720.000	23
2	95.560.000	95.810.000	26 MAL, MRPS5
4	73.920.000	74.120.000	21 COX18, ANKRD17
5	45.060.000	45.290.000	24 HCN1
6	97.800.000	98.010.000	22
7	87.280.000	87.480.000	21 RUNDC3B, SLC25A40
8	99.600.000	99.950.000	36 7SK
11	66.380.000	66.590.000	22 RBM14, RBM4, RBM14-RBM4, RBM4B, SPTBN2, C11orf80

TABLE S2 Contiguous regions of Tajima's D reduction (CRTR) in African populations.

Coordinates (hg19)	Windows	Known genes (UCSC)
CEU		
7	151.770.000 152.080.000	32 GALNT11, MLL3
8	35.560.000 35.830.000	28 UNC5D, AK092313
11	66.890.000 67.140.000	26 KDM2A, DKFZp434M1735, ADRBK1, AK057681, ANKRD13D, SSH3, POLD4, 7SK, CLCF1, LOC100130987
15	44.240.000 44.440.000	21
15	44.580.000 44.890.000	32 CASC4, CTDSPL2, LOC645212, EIF3J, SPG11
15	72.610.000 72.870.000	27 HEXA, C15orf34, TMEM202, ARIH1
17	58.340.000 58.570.000	24 C17orf64, L32131, APPBP2
FIN		
1	35.680.000 36.120.000	45 AF119915, ZMYM4, KIAA0319L, NCDN, TFAP2E, PSMB2
6	95.480.000 95.700.000	23
10	74.790.000 75.250.000	47 NUDT13, BC069792, SNORA11, ECD, FAM149B1, DNAJC9, MRPS16, C10orf103, BC033983, TTC18, ANXA7, ZMYND17, PPP3CB
12	89.020.000 89.230.000	22
GBR		
1	27.930.000 28.140.000	22 FGR, IFI6, FAM76A, STX12
1	35.680.000 36.110.000	44 AF119915, ZMYM4, KIAA0319L, NCDN, TFAP2E, PSMB2
4	33.420.000 33.620.000	21
4	71.580.000 71.850.000	28 RUFY3, GRSF1, MOB1B
8	35.580.000 35.830.000	26 UNC5D, AK092313
11	66.890.000 67.140.000	26 KDM2A, DKFZp434M1735, ADRBK1, AK057681, ANKRD13D, SSH3, POLD4, 7SK, CLCF1, LOC100130987
12	89.020.000 89.210.000	20
16	66.990.000 67.260.000	28 CES3, CES4A, Metazoa_SRP, CBFB, C16orf70, B3GNT9, BC007896, TRADD, FBXL8, HSF4, NOL3, KIAA0895L, EXOC3L1, E2F4, MIR328, ELMO3, LRRC29
17	58.490.000 58.770.000	29 C17orf64, L32131, APPBP2, PPM1D, BCAS3
TSI		
1	35.690.000 36.110.000	43 AF119915, ZMYM4, KIAA0319L, NCDN, TFAP2E, PSMB2
2	182.610.000 182.800.000	20 SSFA2
8	35.600.000 35.850.000	26 AK092313
8	42.720.000 43.000.000	29 MIR4469, HOOK3, FNTA, SGK196, HGSNAT
10	75.130.000 75.350.000	23 ANXA7, ZMYND17, PPP3CB, BC080555, USP54, U6
16	67.040.000 67.300.000	27 Metazoa_SRP, CBFB, C16orf70, B3GNT9, BC007896, TRADD, FBXL8, HSF4, NOL3, KIAA0895L, EXOC3L1, E2F4, MIR328, ELMO3, LRRC29, TMEM208, FHOD1, AK021876, SLC9A5
17	58.500.000 58.770.000	28 L32131, APPBP2, PPM1D, BCAS3

TABLE S3 Contiguous regions of Tajima's D reduction (CRTR) in European populations.

Coordinates (hg19)		Windows	Known genes (UCSC)
CHB			
1	92.570.000	92.950.000	39 KIAA1107, C1orf146, GLMN, RPAP2, GF11
2	72.410.000	72.950.000	55 U2, EXOC6B
2	108.980.000	109.550.000	58 SULT1C4, GCC2, FLJ38668, LIMS1, RANBP2, CCDC138, EDAR
5	117.390.000	117.620.000	24 BC044609
6	126.660.000	126.910.000	26 CENPW, AK127472
11	60.920.000	61.140.000	23 PGA3, PGA4, PGA5, VWCE, DDB1, DAK, CYBASC3, TMEM138
12	44.650.000	44.870.000	23
16	48.120.000	48.410.000	30 ABCC12, ABCC11, LONP2, SIAH1, LOC100507577, MIR548AE2
16	67.220.000	67.580.000	37 E2F4, MIR328, ELMO3, LRRC29, TMEM208, FHOD1, AK021876, SLC9A5, PLEKHG4, KCTD19, LRRC36, U1, TPPP3, ZDHHC1, HSD11B2, ATP6V0D1, AGRP, FAM65A
20	30.190.000	30.390.000	21 ID1, MIR3193, COX4I2, BCL2L1, TPX2
CHS			
2	72.450.000	73.010.000	57 U2, SNORD78, EXOC6B
3	17.340.000	17.860.000	53 TRNA_Pseudo
3	25.880.000	26.110.000	24 LOC285326
5	117.380.000	117.620.000	25 BC044609
8	67.500.000	68.140.000	65 LOC645895, VCPIP1, C8orf44, PTTG3P, C8orf44-SGK3, SGK3, C8orf45, SNORD87, SNHG6, TCF24, U2, PPP1R42, JA611241, COPS5, CSPP1, ARFGEF1
11	60.930.000	61.170.000	25 PGA3, PGA4, PGA5, VWCE, DDB1, DAK, CYBASC3, TMEM138, TMEM216
16	67.240.000	67.530.000	30 LRRC29, TMEM208, FHOD1, AK021876, SLC9A5, PLEKHG4, KCTD19, LRRC36, U1, TPPP3, ZDHHC1, HSD11B2, ATP6V0D1, AGRP
JPT			
1	87.350.000	87.540.000	20 HS2ST1
2	72.410.000	73.080.000	68 U2, SNORD78, EXOC6B
7	142.680.000	142.980.000	31 OR9A2, OR6V1, OR6W1P, PIP, TAS2R39, TAS2R40, GSTK1
12	123.980.000	124.270.000	30 MIR3908, TMED2, DDX55, EIF2B1, GTF2H3, TCTN2, ATP6V0A2, DNAH10
13	20.190.000	20.440.000	26 MPHOSPH8, PSPC1, ZMYM5
16	48.110.000	48.380.000	28 ABCC12, ABCC11, LONP2, MIR548AE2
16	67.230.000	67.590.000	37 MIR328, ELMO3, LRRC29, TMEM208, FHOD1, AK021876, SLC9A5, PLEKHG4, KCTD19, LRRC36, U1, TPPP3, ZDHHC1, HSD11B2, ATP6V0D1, AGRP, FAM65A

TABLE S4 Contiguous regions of Tajima's D reduction (CRTR) in Asian populations.

Coordinates (hg19)		Windows	Known genes (UCSC)
ASW			
1	26.990.000	27.240.000	26 ARID1A, PIGV, ZDHHC18, SFN, GPN2, GPATCH3, NR0B2, BC016143
2	95.560.000	95.760.000	21 MAL, MRPS5
4	93.690.000	93.930.000	25 GRID2
4	145.910.000	146.130.000	23 ANAPC10, ABCE1, OTUD4, Mir_649
5	45.060.000	45.280.000	23 HCN1
16	46.470.000	46.660.000	20 ANKRD26P1, SHCBP1
20	20.460.000	20.750.000	30
22	28.400.000	28.740.000	35 Y_RNA
LWK			
1	41.500.000	41.710.000	22
3	93.670.000	93.860.000	20 ARL13B, STX19, DHFRL1, NSUN3, U7
4	87.390.000	87.620.000	24 PTPN13
8	99.600.000	99.930.000	34
11	66.390.000	66.590.000	21 RBM14, RBM4, RBM4B, SPTBN2, C11orf80
12	87.490.000	87.680.000	20
17	44.210.000	44.400.000	20 LOC644246, ARL17A, LRRC37A
YRI			
1	41.490.000	41.720.000	24 SCMH1
2	95.560.000	95.850.000	30 MAL, MRPS5, ZNF514, ZNF2
5	45.070.000	45.290.000	23 HCN1
6	97.800.000	97.990.000	20
8	99.600.000	99.950.000	36 7SK
11	66.380.000	66.620.000	25 RBM14, RBM4, RBM14-RBM4, RBM4B, SPTBN2, C11orf80, RCE1, PC

TABLE S5 Contiguous regions of Tajima's D (demography-adjusted) reduction (CRTR) in African populations

Coordinates (hg19)		Windows	Known genes (UCSC)
CEU			
1	35.720.000	35.920.000	21 AF119915, ZMYM4, KIAA0319L
7	87.270.000	87.510.000	25 RUNDC3B, SLC25A40, DBF4
7	151.770.000	152.080.000	32 GALNT11, MLL3
8	35.570.000	35.840.000	28 UNC5D, AK092313
11	66.880.000	67.140.000	27 KDM2A, DKFZp434M1735, ADRBK1, AK057681, ANKRD13D, SSH3, POLD4, 7SK, CLCF1, LOC100130987
13	72.070.000	72.270.000	21
15	44.240.000	44.430.000	20
15	44.570.000	44.800.000	24 CASC4, CTDSPL2
15	72.610.000	72.890.000	29 HEXA, C15orf34, TMEM202, ARIH1, MIR630
17	58.340.000	58.570.000	24 C17orf64, L32131, APPBP2
FIN			
1	35.680.000	36.120.000	45 AF119915, ZMYM4, KIAA0319L, NCDN, TFAP2E, PSMB2
3	96.470.000	96.660.000	20 EPHA6
6	95.480.000	95.710.000	24
8	48.660.000	48.910.000	26 PRKDC, MCM4
12	89.020.000	89.230.000	22
16	47.190.000	47.520.000	34 Y_RNA, ITFG1, PHKB
GBR			
1	35.680.000	36.110.000	44 AF119915, ZMYM4, KIAA0319L, NCDN, TFAP2E, PSMB2
4	33.420.000	33.610.000	20
6	128.440.000	128.650.000	22 PTPRK
8	35.580.000	35.850.000	28 UNC5D, AK092313
8	67.660.000	67.950.000	30 PTTG3P, SGK3, C8orf45, SNORD87, SNHG6, TCF24, U2, PPP1R42
11	66.890.000	67.140.000	26 KDM2A, DKFZp434M1735, ADRBK1, AK057681, ANKRD13D, SSH3, POLD4, 7SK, CLCF1, LOC100130987
16	66.970.000	67.260.000	30 CES3, CES4A, Metazoa_SRP, CBF, C16orf70, B3GNT9, BC007896, TRADD, FBXL8, HSF4, NOL3, KIAA0895L, EXOC3L1, E2F4, MIR328, ELMO3, LRRC29
17	58.490.000	58.780.000	30 C17orf64, L32131, APPBP2, PPM1D, BCAS3
TSI			
1	35.690.000	36.110.000	43 AF119915, ZMYM4, KIAA0319L, NCDN, TFAP2E, PSMB2
4	33.430.000	33.620.000	20
8	35.570.000	35.860.000	30 UNC5D, AK092313
8	42.720.000	43.000.000	29 MIR4469, HOOK3, FNTA, SGK196, HGSNAT
16	67.040.000	67.310.000	28 Metazoa_SRP, CBF, C16orf70, B3GNT9, BC007896, TRADD, FBXL8, HSF4, NOL3, KIAA0895L, EXOC3L1, E2F4, MIR328, ELMO3, LRRC29, TMEM208, FHOD1, AK021876, SLC9A5
17	58.520.000	58.770.000	26) APPBP2, PPM1D, BCAS3

TABLE S6 Contiguous regions of Tajima's D (demography-adjusted) reduction (CRTR) in European populations

Coordinates (hg19)		Windows	Known genes (UCSC)
CHB			
1	92.570.000	92.950.000	39 KIAA1107, C1orf146, GLMN, RPAP2, GFII
2	72.410.000	72.950.000	55 U2, EXOC6B
2	108.980.000	109.440.000	47 SULT1C4, GCC2, FLJ38668, LIMS1, RANBP2, CCDC138
5	117.390.000	117.620.000	24 BC044609
6	126.660.000	127.030.000	38 CENPW, AK127472, Vimentin3
11	60.920.000	61.150.000	24 PGA3, PGA4, PGA5, VWCE, DDB1, DAK, CYBASC3, TMEM138
12	44.590.000	44.880.000	30
16	47.090.000	47.410.000	33 NETO2, Y_RNA, ITFG1
16	47.510.000	48.410.000	91 PHKB, BC048130, ABCC12, ABCC11, LONP2, SIAH1, LOC100507577, MIR548AE2
16	67.190.000	67.850.000	67 FBXL8, HSF4, NOL3, KIAA0895L, EXOC3L1, E2F4, MIR328, ELMO3, LRRC29, TMEM208, FHOD1, AK021876, SLC9A5, PLEKHG4, KCTD19, LRRC36, U1, TPPP3, ZDHHC1, HSD11B2, ATP6V0D1, AGRP, FAM65A, CTCF, DL491203, RLTPR, ACD, PARD6A, C16orf48, C16orf86, AX747090, GFOD2, RANBP10, TSNAXIP1
20	30.120.000	30.370.000	26 PSIMCT-1, HM13, ID1, MIR3193, COX4I2, BCL2L1, TPX2
CHS			
2	72.450.000	73.020.000	58 U2, SNORD78, EXOC6B
2	82.540.000	82.810.000	28
3	17.350.000	17.830.000	49 TRNA_Pseudo
5	117.390.000	117.620.000	24 BC044609
6	126.660.000	127.020.000	37 CENPW, AK127472, Vimentin3
8	67.600.000	68.140.000	55 PTTG3P, SGK3, C8orf45, SNORD87, SNHG6, TCF24, U2, PPP1R42, JA611241, COPS5, CSPP1, ARFGEF1
10	22.030.000	22.280.000	26 DNAJC1, 7SK
11	60.930.000	61.200.000	28 PGA3, PGA4, PGA5, VWCE, DDB1, DAK, CYBASC3, TMEM138, TMEM216, CPSF7, SDHAF2
12	88.480.000	88.760.000	29 CEP290, TMTC3
16	47.080.000	47.410.000	34 NETO2, Y_RNA, ITFG1
16	47.430.000	48.140.000	72 ITFG1, PHKB, BC048130, ABCC12
16	67.230.000	67.910.000	69 MIR328, ELMO3, LRRC29, TMEM208, FHOD1, AK021876, SLC9A5, PLEKHG4, KCTD19, LRRC36, U1, TPPP3, ZDHHC1, HSD11B2, ATP6V0D1, AGRP, FAM65A, CTCF, DL491203, RLTPR, ACD, PARD6A, C16orf48, C16orf86, AX747090, GFOD2, RANBP10, TSNAXIP1, CENPT, THAP11, NUTF2, EDC4

TABLE S7 Contiguous regions of Tajima's D (demography-adjusted) reduction (CRTR) in Chinese populations

Coordinates (hg19)		Windows	Known genes (UCSC)
JPT			
1	27.000.000	27.320.000	33 ARID1A, PIGV, ZDHHC18, SFN, GPN2, GPATCH3, NR0B2, NUDC, C1orf172, BC016143
1	92.570.000	93.180.000	62 KIAA1107, C1orf146, GLMN, RPAP2, GFI1, EVI5
2	72.410.000	73.080.000	68 U2, SNORD78, EXOC6B
6	126.660.000	127.030.000	38 CENPW, AK127472, Vimentin3
7	142.680.000	142.980.000	31 OR9A2, OR6V1, OR6W1P, PIP, TAS2R39, TAS2R40, GSK1
12	124.010.000	124.270.000	27 MIR3908, TMED2, DDX55, EIF2B1, GTF2H3, TCTN2, ATP6V0A2, DNAH10
13	20.230.000	20.430.000	21 PSPC1, ZMYM5
16	46.900.000	48.400.000	151 GPT2, DNAJA2, NETO2, Y_RNA, ITFG1, PHKB, BC048130, ABCC12, ABCC11, LONP2, SIAH1, LOC100507577, MIR548AE2
16	67.180.000	67.750.000	58 B3GNT9, BC007896, TRADD, FBXL8, HSF4, NOL3, KIAA0895L, EXOC3L1, E2F4, MIR328, ELMO3, LRRC29, TMEM208, FHOD1, AK021876, SLC9A5, PLEKHG4, KCTD19, LRRC36, U1, TPPP3, ZDHHC1, HSD11B2, ATP6V0D1, AGRP, FAM65A, CTCF, DL491203, RLTPR, ACD, PARD6A, C16orf48, C16orf86, AX747090, GFOD2

TABLE S8 Contiguous regions of Tajima's D (demography-adjusted) reduction (CRTR) in the Japanese population